Powerful Advanced N-Level Digital Architecture
for models of electrified vehicles and their components

https://project-panda.eu/

Research Innovation Action

GA # 824256

EUROPEAN COMMISSION
Horizon 2020 | GV-02-2018
Virtual product development and production of
all types of electrified vehicles and components

Deliverable No.	PANDA D4.3	
Deliverable Title	Report on the virtual testing of the BEV	
Deliverable Date	2020-11-30	
Deliverable Type	REPORT	
Dissemination level	Public (PU)	
Written By	Gabriel SIRBU (RTR) Anatole DESREVEAUX (ULille) Calin HUSAR (SISW) Niculae BOICEA (RTR)	2021-01-26
Checked by	Cristi IRIMIA (SISW)	2021-02-01
Approved by	Calin HUSAR (SISW) Johannes ROESSNER (TUV) Alain BOUSCAYROL (ULille) - Coordinator	2021-02-01 2021-02-01 2021-02-01
Status	Final	2021-02-01

Publishable Executive Summary

PANDA project has the objective to provide a disruptive and open-access model organisation for system simulation and whole vehicle simulation with the goal to reduce the time to market for electrified vehicles. Simulation is more and more used in vehicle development and this tool is in a continuous transformation as the digital technologies and capabilities are in a fast-growing period. The big advantage of the use of simulations during development of a product is the reduced time for evaluation of the performance of the product, in our case the evaluation of the performance of vehicle systems and global vehicle performances. So, improving simulations will lead to a faster vehicle development, a cost reduction of the development and a cost optimisation of the vehicle.

The methodology for model organisation proposed in PANDA project is based on the EMR (Energetic Macroscopic Representation) formalism as a graphical guideline. Using this formalism, PANDA partners have developed models for main subsystems of an electrified vehicle and a global model of the vehicle was built with these models. The purpose of this report is to present the validation of the models of Battery Electric Vehicle (BEV) and to prove the performance of the methodology proposed by using multi-level models.

One of the features of the proposed methodology is the flexibility of the simulation given by the possibility of seamless replacing of a model of a component or a subsystem with another model of the same component or subsystem but with a different complexity. This feature gives the possibility to change very easily the simulation type one can perform on the same global architecture. A quick replacement of a model and some tuning on simulation parameters can provide a simulation for a system validation or a simulation for the validation of a global performance of the vehicle. In this report, besides the validation of global vehicle simulation, it is tested the flexibility of the simulation architecture when models are changed.

Simulation results for the global traction system of a BEV are compared with physical measurements performed on the real vehicle. Renault ZOE Q90 was the BEV chosen for tests and the vehicle was tested in Titu Technical Centre from Renault Technologie Roumanie (RTR). Simulations are performed using Matlab-Simulink© software and Simcenter Amesim© software provided by the partner SISW. Different complexity models for electrical battery developed by VUB and electrical drive developed by UTCN are presented and implemented in both software solutions using the EMR model organisation. Validation of global vehicle simulation was done by ULille. Multi-level simulations of global vehicle were done by SISW and parameters from simulation are compared with experimental results from the real vehicle. Thus, the accuracy and efficiency of different simulations was proved, and the model organization capability was demonstrated. The test scenarios for the validation of simulations were chosen to cover the normal usage of a vehicle with urban cycles, mixed cycles and highway cycles.

The comparison of the simulated results with measured results was done to evaluate the performance of the different models regarding of precision of the results and simulation time. This last aspect is necessary to be evaluated because the next step in PANDA project is the integration of models in real-test HIL testing.

Contributions:

No	*Who*	*Description*	*Date*
1	G. SIRBU(RTR), A. BOUSCAYROL (ULille)	Report creation and outline	2020-11-20
2	G. SIRBU, N. BOICEA (RTR),	Section 1	2020-11-22
3	A. DESREVEAUX (ULille), G. SIRBU (RTR)	Section 2, 3, 4	2020-11-24
4	J. JAGUEMONT (VUB)	Section 5.1	2019-11-29
5	M. RAIA (UTCN)	Section 5.2	2020-11-27
6	E. RACLARU (SISW), A. DESREVEAUX (ULille)	Section 5.3	2020-11-24
7	C. HUSAR, E. RACLARU (SISW), G. SIRBU (RTR)	Section 5.4	2020-12-04
8	A. BOUSCAYROL(ULille), A.TINTELECAN(UTCN), M.KOROMA(VUB)	Section 6	2021-01-16
9	G. SIRBU (RTR)	Update and conclusions	2021-01-26
10	G. SIRBU (RTR)	Finalization	2021-01-26

Contents

Figures

Tables

1. Introduction

The objective of PANDA project is to provide a disruptive and open access model organization for an easy interconnection and change of models in the development process of electrified vehicles [PANDA 2019]. The model organisation is based on EMR (Energetic Macroscopic Representation) formalism [Bouscayrol 2012]. The formalism is implemented in the 1D simulation tools, Matlab-Simulink© and Simcenter Amesim©, an industrial simulation tool used in automotive industry. The models necessary for building a vehicle simulation were developed by the PANDA partners. They developed multi-scale multi-domain models based on EMR formalism that can be introduced in a simulation architecture of an electrified vehicle.

This report is dedicated to a battery electric vehicle (BEV) simulation and validation of vehicle simulation using the EMR formalism by comparing simulation results with experimental tests on a real vehicle. The vehicle measured was Renault ZOE Q90 produced by Renault and tested in Titu Technical Center of RTR – Romania. For this purpose, the models were tuned using data provided by RTR in order to be adapted to the tested vehicle.

The models were developed during previous stages of the project as follows:

- In Work Package 2 (WP2) – work package leader VUB, battery models were developed
- In Work Package 3 (WP3) – work package leader UTCN, electric drives models were developed
- In Work Package 4 (WP4) – work package leader SISW, car body model was developed

All models were implemented in Simcenter Amesim© by SISW, the owner of the simulation tool.

The simulation architecture of Renault ZOE was implemented in Matlab-Simulink© by ULille and in Simcenter Amesim© by SISW following the EMR formalism; thus there was built a simulation platform as it was set by project objectives. This simulation platform was put in common for all partners using a cloud solution also implemented by SISW.

The tests performed on the BEV were decided according to the study form Work Package 1 (WP1) – work package leader UBFC, and specific demands form partners who developed individual models. The test scenarios are adapted for the validation of individual models and validation of the global vehicle performances.

A multi-level simulation of the BEV studied vehicle is performed in Simcenter Amesim©. The results of these simulations are compared with measured results and prove the efficiency and flexibility of the simulation platform developed in the PANDA project. This report presents different models adapted to the BEV tested. The subsystem models used in such configuration are replaced by other models of the same subsystems built with a different complexity. These models with the same input and output parameters are used in the same simulation architecture. Using this technique, it is validated the flexibility of the platform and the models can be compared directly having the same test conditions for simulation and for the real driving cycles.

The simulation results are close to the experimental results on the real vehicle in all configurations and this fact gives confidence that the objective of the PANDA project (to provide a unified organisation of digital models for seamless integration in virtual testing for a BEV) is achieved.

1.1 Battery Electric Vehicle (BEV) description

The Battery Electric Vehicle (BEV) is the type of vehicle that uses only the chemical energy stored in a battery for the propulsion. No other secondary source of energy is used for the propulsion. That means no combustion engine, no fuel cell, no other source of electrical or mechanical energy is used in this vehicle for propulsion or to charge the battery.

The energy from the battery is transfer to one or several electrical drives who transforms the electrical energy to mechanical energy used for propulsion of the vehicle. The electrical drives are controlled by motor controllers to provide the necessary torque for the vehicle. The assembly of the electrical machine, power converter (i.e. inverter) and controller is called electrical drive (e-drive) and for smaller power it is manufactured as single unit component. As this BEV is a medium power application the e-drive has a separate motor controller.

With the actual level of technology for batteries and electrical drives almost all types of vehicles have a battery electric type: cars, buses, bicycles, scooters, railcars, watercrafts, forklifts etc. The limitation of the

use of battery electric vehicles is done by the battery capacity and costs. For high power applications of electrical vehicles there are not affordable batteries yet, but as battery technology is developing, these limits change every year, for example electrical buses are used since 1992 and battery electrical railcars started in 2014. This technology is popular for small power vehicles and is already competing on passenger car and buses segment.
In the PANDA project, a small passenger car was considered for BEV, Renault ZOE, one of the most popular electric cars in Europe (Figure 1)

Figure 1 Renault ZOE

An electric car has usually the e-drive inside the engine compartment, but there are solutions with e-drives integrated in the vehicle wheels. The electrical machine is coupled to the wheels with a single-ratio gearbox and the entire electrical drive module is smaller and lighter than a conventional fuel engine with a conventional multi-ratio gearbox. Thus, there is place for other specific components of a BEV: battery charger and auxiliary converter necessary for powering all electrical systems of a car: lights, electric control units (ECUs), windshield wipers, HVAC, etc. In Renault ZOE, all electrical converters (battery charger, inverter and auxiliary consumer converter) are packed in one component called Power Electronics Block (PEB).

The electrical battery is the biggest and heaviest component of a BEV. For a Renault ZOE car it is 305kg (for 1.4-ton vehicle). Placing such a weight in a car is difficult and has a big influence in the architecture of the car. Usually the best place of the battery is under the car floor for dynamical performance of the car and smallest influence on architectural space (Figure 2).

Figure 2 Typical structure of the powertrain of Renault ZOE

The high-power circuit between the battery, the e-drive, the battery charger and the charging plug must be well insulated and protected. As the car is not connected to the ground, the high-power electrical circuit is carefully designed.
Automotive environment is different from industrial environment and all electrical components of the car are designed according to automotive standards. These standards have larger temperature domains, higher corrosion conditions and higher vibrations than industrial standards. This is the reason why electrical components for BEVs are more expensive than similar industrial ones. Besides they have control modules with complex functions implemented for safety and maximal performance from efficiency point of view. The design of these components and subsystems and the validation in a BEV's environment is a complex process, expensive and time consuming.
Hence, the PANDA project objectives can help to reduce the cost and the time of the design and validation of these components.
Figure 3 presents the diagram of the main components of the BEV Renault ZOE. In this figure there is the green circuit which is the high-power circuit fed by the battery between the main components and the purple circuit a small high-power circuit between the inverter and the electrical machine. The circuit battery-inverter-electrical machine is the main part of the electrical powertrain. This powertrain provides the torque necessary to move the car. The car body with the wheels and transmission chain represent the bi-directional power source for the electrical powertrain (i.e. for the traction and regenerative braking modes). These are the subsystems studied and validated in this report and this is the considered electrical architecture of the BEV.

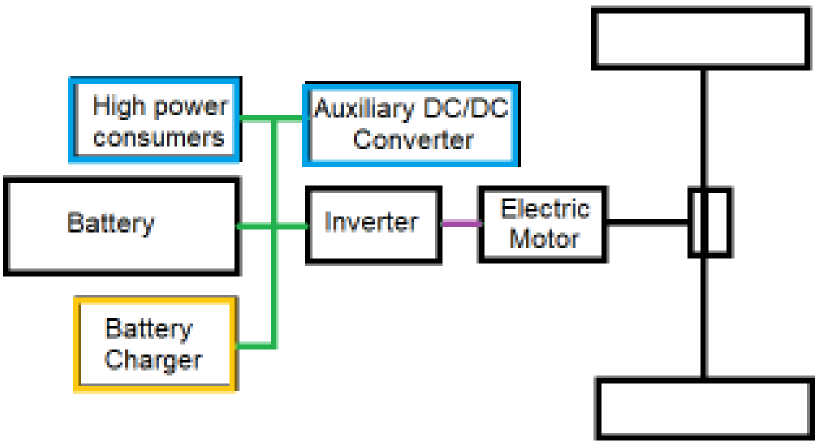

Figure 3 Electrical diagram of the powertrain of a BEV

1.2 Test methodology for model validation

The testing methodologies used to perform the tests on the real vehicle, Renault ZOE, were defined based on report [PANDA D1.6] and the specific needs from partners in charge with development of models. According to the specificity of each subsystem, several scenarios were chosen to be measured which can cover the demands for all the partners.
All modelled subsystems must be able to be used for simulation of their own performances and to be available to be used in the global vehicle simulation for global performance of the vehicle. For this reason, the tests were done with a real vehicle.
A car Renault ZOE Q90 was used for the experimental tests. This is a car on the market since 2017 and is representative from the point of view of the level of technology used. It is a BEV at the average level of the market from this point of view. General data for the car and for the electric powertrain is in Table 1.

Table 1 Technical specification of Renault ZOE Q90 used for tests

Body style	Hatchback	Electrical machine	Synchronous with rotor coil
Number of seats	5	e-machine max power (kW/hp) at maximum rpm	65/88 at 3000-11300
Dimensions LxWxH (mm)	4084 x 1730 x 1562	e-machine peak torque (Nm) at maximum rpm	220 at 250-2500
Wheelbase (mm)	2588	Battery Technology	Lithium-ion
Weight (kg)	1480	Total voltage (V)	400
Cargo volume (l)	338	On-board energy (kWh)	41
Top speed (km/h)	135	Charger	Adaptable for single or three-phase power 2-43kW
Acceleration 0-100km/h (s)	13,2	Autonomy NEDC (km)	370

The tests were performed in Titu Technical Center of RTR in Romania. This is the largest test center from Easter Europe for automotive industry. Titu Technical Center has the mission of testing cars and mechanical parts, especially those from the Global Access range (Logan, Sandero, Duster), manufactured worldwide. Inaugurated on September 15th, 2010, the Titu Technical Center is the 2nd testing center, in terms of size, of the Renault Group worldwide and it has an area of 350 ha. Its staff work with the most recent testing technologies and machines for cars and parts, in various phases of development projects, but also in the most diverse climate and road conditions. Titu Technical Center has a network of tracks, unique in the region, with a total length of 32 km that enables the in-depth analysis of the smallest details related to how cars behave in diverse roads and driving conditions. Ten types of tracks, among which the rapid track, the city track, the slope track, the cobblestone track, the wet handling circuits which all simulate difficulties a driver may encounter from rural roads to big city traffic or highways. The major advantage of the testing facilities from Titu is that in a very short time they can simulate an intensive use, equivalent of that of many years for a real client.
Titu Technical Center buildings host dozens of testing benches for cars, for parts of the car, but also for mechanical parts (engines, gearboxes). Similarly, to the tracks, they reproduce driving situations in extreme conditions: very high or low temperatures, wind, etc. The car, or some of its parts, are tested for hours in sun or cold simulators, in booths with different rain intensities or they run on benches that test their clutch, their gearshift, etc.

Figure 4 Titu Technical Center of RTR - Romania

Models must reproduce the behaviour of the systems for normal use of a vehicle so, there were chosen cycles of use from real life. For an average user of a car, most of the time she/he uses the car in urban areas for daily activities. There are cases when the user has some extra urban parts from her/his routes and some stationary periods. As a separate cycle, a highway test was performed. This is a very important test for BEV because here are tested the limitations of the vehicle in terms of normal use. The energy consumption is maximum during highway use and there are few possibilities to optimize this consumption. All electrical parts (battery, inverter, electrical machine) are pushed to their thermal limits.

The following scenarios were tested on chosen vehicle – Renault ZOE:

- An urban cycle in a large city with intense traffic – measured in the city of Bucharest/Romania
- A mixed urban and extra urban cycle with less intense traffic – measured in a small town
- A highway cycle with speed variation – measured on the real highway - Bucharest-Pitesti
- Several acceleration-braking cycles on a flat area – measured on dedicated tracks

As mentioned before the simulation of subsystems working together in a vehicle environment must be validated for short time use and for long time use. The vehicle must not be modified or charged with additional masses and the electrical network of the vehicle must not have additional consumers. For such reasons the measurements were done using sensors and electronic control units (ECUs) that are present on the vehicle. Information from sensors is treated by several ECUs that are in charge with the management of the systems in the vehicle.

The main ECUs used for measuring data on the vehicle were:

- for battery management, it is Battery Management System (BMS)
- for inverter it is Power Electronics Block (PEB) control unit
- for global coordination of electrical powertrain, it is Electric Vehicle Computer (EVC)

Internal transmissions speed, computing speed and output transmission speed are factors that affects the sampling time of the measurements. A detailed analysis was done to obtain the necessary list of variables to be measured from several ECUs in order to have an optimized sample time. The optimized sample time was 1sample/second (1 Hz) with all variables measured in the same time.

The cycles were long enough to measure and evaluate the total energy consumption of the car – a very important variable because it is necessary to evaluate the autonomy of the car – the key performance of a BEV today.

Here are the graphics of vehicle speed with a short description of tests performed.

In urban cycle, there are many acceleration and braking and the recovered energy from braking is important. There are also constant speed periods appropriated to evaluate the steady state behaviour of models. Comparing with standard cycles, such as NEDC or WLTP, the accelerations and breakings are relevant for the way a European driver acts. As the selected driving cycle is realized in a big city (Bucharest), it can be noted some sections with 120 km/h in some express roads (Figure 5). An intense traffic was observed during this test.

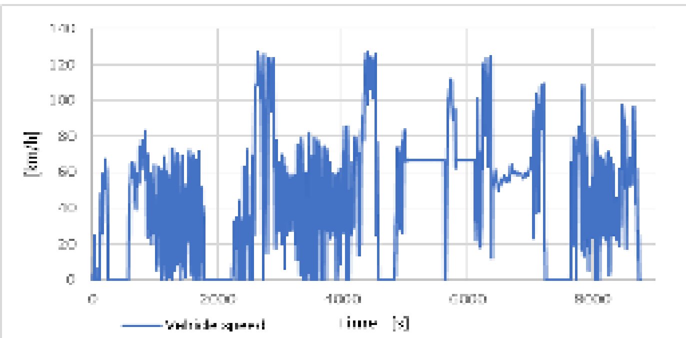

Figure 5 Urban cycle in a large city

During mixed urban and extra urban cycles, there are accelerations and decelerations at higher speeds and longer periods with constant speed. The recovered energy is more important (mechanical brakes less used) and the subsystems are working without limitations (e.g. temperature, speed, current limitations). This testing driving cycles was recorded without intense traffic (Figure 6).

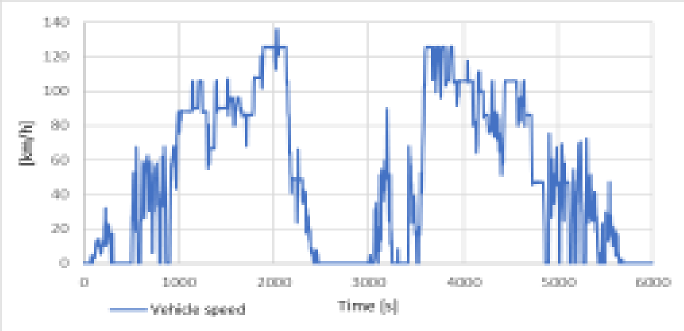

Figure 6 Mixed urban and extra urban cycle

A highway cycle is a driving cycle where the subsystems operates close to their termal and technical limits. The discharge of the battery is quicker than in any other cycle. Electrical losses are easier to be identified. This test driving cycle has been recorded between Bucharest and Pitesti with a normal traffic (Figure 7).

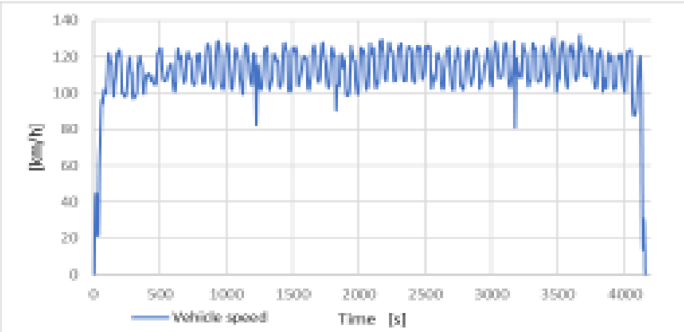

Figure 7 Highway cycle with speed variation

1.3 Organisation method of the models for virtual testing

The organisation method for virtual and real testing defines the methodology requirements for the development of multi-level model organization for the PANDA objective. The method was described in report [PANDA D1.2]. The method imposes the following lines to be respected during the design and construction of the simulation platform:

- For models: different models are defined for the same subsystem according to the objective of the study. In PANDA, a multi-level model approach is targeted to develop a N-level model organization. For the same subsystem, different models will thus be developed. Dynamical models (for transient states), static models (only for steady states) and quasi-static models are considered.
- For representation: in the PANDA project, a functional description is imposed to avoid the need of co-simulation. Moreover, this choice enables to use pure causal description (i.e. physical causality, i.e. integral causality) [Hautier 2004] that leads to the reduction of the computation time [Rubin 1997]. The EMR (Energetic Macroscopic Representation) formalism [Bouscayrol 2012] is selected.
- For simulation: most of the actual advanced simulation packages are defined in structural philosophy as explained in the previous paragraph [PANDA D1.1]. In the PANDA project, the functional approach used is a challenging task, which requires some adaptation of actual simulation packages. Forward and backward approaches are used in function of the global objective. The forward approach is more dedicated for control development and real-time simulation using dynamical models. The backward approach is more used for design and global energetic studies using static and/or quasi-static models.

The EMR formalism is selected for the unified models' organisation because it is a graphical formalism (synthetic and unified view) based on a functional approach (flexibility) using exclusively the natural physical

causality (adapted for real-time). Association rules have been defined in EMR for solving conflict of association. This property enable a systematic deduction of the control organization of the studied system by an inversion of the system EMR.
In order to organise the model of energy conversion systems for control purpose, only 4 energetic functions are sufficient [Bouscayrol 2012]: source of energy, storage of energy, conversion of energy and distribution of energy. EMR is thus based on basic pictograms to describe these functions (Table 2). Other pictograms have been defined to manipulate the models: switching between two models and power amplification to avoid model repetition, and 3 pictograms for controls (blue pictograms).

Table 2 EMR elements

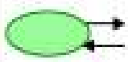	Source element (energy source)		Accumulation element (energy storage)		Indirect inversion (closed-loop control)
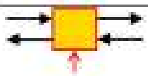	Mono-physical conversion element	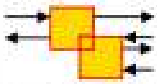	Mono-physical coupling element (energy distribution)		Direct inversion (open-loop control)
	Multi-physical conversion element		Multi-physical coupling element (energy distribution)	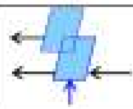	Coupling inversion (energy criteria)

The EMR of the complete system is thus composed of the connected EMR elements after solving the different conflicts of association using the permutation and merging rules.
In the PANDA project, each partner developed the models of subsystems she/he is in charge with, using her/his own software solution (e.g. Matlab-Simulink©). These models are developed using the EMR formalism and they were validated with physical measurements. After that, the models are translated in Simcenter Amesim© with the help of SISW who developed an EMR library with elements according to EMR rules for an easier implementation [PANDA D4.1].

2. Modelling and representation of the studied BEV

The modelling of the BEV is following the typical structure of a BEV (see Figure 3). The main power transfer of the energy from battery to the wheels is modelled without the charging system as this is a stand-alone system and is not working during the use of the vehicle. The auxiliary DC/DC converter for low power consumers and high-power consumers are considered as constant auxiliary consumers (Figure 8):

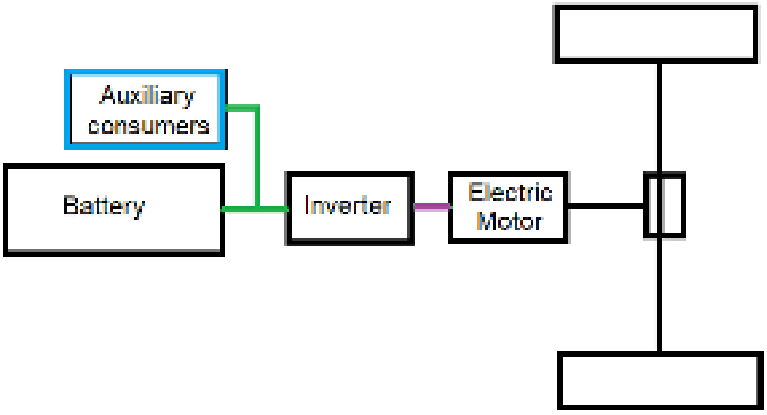

Figure 8 BEV structure for modelling

The model of the BEV is developed using the EMR formalism and using EMR pictograms (see Table 2). Different battery models are considered: a global electrical model (level-0), a cell electrical model and their associations (level-1) and an electro-thermal model (level-2). Different e-drive models are also considered: static efficiency map (level-0), dynamical park model with ideal control (level-1), dynamical model with practical control including estimation (level-2). In this section 2, only level-0 models for battery and e-drive are considered.

The battery voltage u_{bat} depends on the open-circuit voltage (OCV) u_{ocv}, the current i_{bat} and the battery resistance R_{bat}. The OCV depends on the State-of-Charge (SoC) of the battery. The battery is represented as a source element (green oval pictogram, Table 2)

$$u_{bat} = u_{ocv}(SoC) + R_{bat} i_{bat} \tag{1}$$

Equation (1) represents a simple model of a battery as a voltage source depending on SoC and the current. It is considered as a level-0 model for a battery in this report.
The battery is connected to auxiliary consumers and the electric drive (overlapped orange squares, Table 2). The battery current i_{bat} is the sum of the electric drive current and the auxiliary current i_{aux}.

$$i_{bat} = i_{ed} + i_{aux} \tag{2}$$

A static model of the electric drive is considered for this first model (orange circle). The torque of the electric drive T_{ed} depends on the reference torque T_{ed_ref}. The current of the electric drive depends on the electric drive torque T_{ed}, the speed of the gearbox Ω_{gb}, the battery voltage $u_{bat.}$ The efficiency η_{ed} is obtained through a lookup table efficiency map. This level-0 model of the e-drive is expressed by equation (3).

$$\begin{cases} T_{ed} = T_{ed\_ref} \\ i_{ed} = \dfrac{T_{ed} \Omega_{gb} \eta_{ed}(T_{ed},\ \Omega_{gb})}{u_{bat}} \end{cases} \tag{3}$$

The efficiency map table contains in fact recorded output values for known inputs. This static model is a table of steady state points of a system and with such a model, it is not possible to simulate with a good approximation high dynamical transient response. But, for low dynamical responses or quasi static processes, this static model is useful and precise.

This type of model is used for e-drive models to simulate the energy consumption or the mechanical behaviour of the load system. An e-drive subsystem is a high dynamical system with very fast changes of the currents and voltages. To have an accurate simulation of this subsystem, a small sample time must be used. For example in the case of a BEV where the electric machine is fed with PWM voltages with frequencies over 10 kHz (including the generated harmonics), for a detailed simulation one must use a sample time at least 10 times lower than the PWM period, for this case maximum 10 μs. With this sample time, it takes a lot of time to simulate the whole vehicle for calculation the energy consumption during a driving cycle of about an hour. And the precision of such a model, in terms of energy consumption, is not much better than a simulation with a level-0 model with a sample time of 0.5s. The problem of this model is that it is not available until the moment when the e-drive is built, and the efficiency-map values are measured on a test bench. Thus, the static model is available to be implemented on the vehicle before the vehicle is built and the e-drive integrated for vehicle test.
Another case when this model is useful is before the design of the electrical machine and the e-drive. In this case, the general data of the vehicle and transmission are available, and a fast model can be built according to the vehicle torque and speed demands. Once the model is built and tested to fulfil the vehicle performances, it can be used as target for the design of the real electrical machine and e-drive. As consequence as, the level-0 model is interesting to have a fast and accurate simulation in a first step.

The gearbox (conversion element - orange square, Table 2) leads to the gearbox speed Ω_{gb} from the wheel speed Ω_{wh} and the gearbox ratio k_{gb} (see Figure 9). The gearbox torque T_{gb} depends on the electric drive torque T_{ed}, the gearbox ratio k_{gb}, and the gearbox efficiency η_{gb}.

$$\begin{cases} \Omega_{gb} = \Omega_{wh} k_{gb} \\ T_{gb} = T_{ed} k_{gb} \eta_{gb} \end{cases} \tag{4}$$

In the model, it is assumed that the wheels are not affected by slips and turns, so an equivalent wheel is considered (orange square). It transforms the vehicle velocity v_{veh} into wheel speed Ω_{wh} with the wheel radius R_{wh}, and the gearbox torque T_{gb} into the wheel force F_{wh}.

$$\begin{cases} \Omega_{wh} = \frac{v_{veh}}{R_{wh}} \\ F_{wh} = \frac{T_{gb}}{R_{wh}} \end{cases} \tag{5}$$

The wheel force F_{wh} is added to the mechanical braking force F_{br} to give the total force applied to the vehicle F_{tot} in a coupling element (overlapped orange squares, Table 2).

$$F_{tot} = F_{wh} + F_{br} \tag{6}$$

The Newton's second law is used to calculate the velocity of the car v_{veh}, which depends on the total traction force, resistive force to the motion F_{res} and the vehicle mass M_{ev}. An accumulation element (crossed orange rectangle) represents the accumulation of the energy in the chassis.

$$v_{veh} = \frac{1}{M_{ev}} \int (F_{tot} - F_{res}) dt \tag{7}$$

The road environment (green oval) represents the resistive force F_{res} given by the environment. This force is composed of the aerodynamic force F_a, the road resistance force F_r and the slope F_s.

$$F_{res} = F_a + F_r + F_s \tag{8}$$

From the EMR of a studied system, an inversion-based control scheme can be systematically obtained. Relation (7) is inverted by a closed-loop control (crossed blue parallelogram).

$$F_{tot-ref} = C(t)(v_{veh-ref} - v_{veh}) + F_{res} \tag{9}$$

with *C(t)* a controller to be defined. Relation (6) is next inverted using a distribution input k_D(t) to distribute the forces between the brakes and the wheel.

$$\begin{cases} F_{br-ref} = k_D F_{tot-ref} \\ F_{wh-ref} = (1-k_D)F_{tot-ref} \end{cases} \tag{10}$$

In the traction mode, k_D=0 (no braking force). In the braking mode, k_D=0.5 to equally distribute the braking force between the brakes and the electric drive. Moreover, a limitation curve of the electric drive is used to limit its torque as a function of the rotation speed. The distribution input k_D is calculated in the strategy block, where more advanced braking strategies can be defined [Qiu 2016].
Relations (5) are directly inverted to obtain the gearbox torque reference.

$$T_{gb-ref} = R_{wh}F_{wh-ref} \tag{11}$$

Finally, equation (4) is directly inverted to obtain the electric drive torque reference $T_{ed\text{-}ref}$, the control reference for the e-drive.

$$T_{ed-ref} = \frac{1}{k_{gb}} T_{gb-ref} \tag{12}$$

The EMR model organization of the BEV is presented in Figure 9.

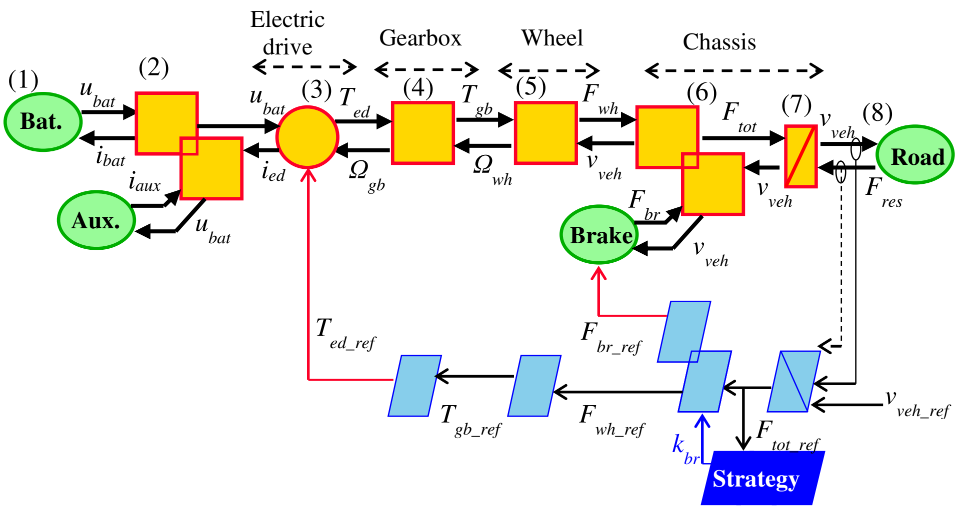

Figure 9 EMR of the studied BEV

3. Simulation and validation of the studied BEV using Matlab-Simulink©

The efficiency map of the e-drive of the Renault ZOE car is presented in Figure 10. It can be noticed that it has a high efficiency in a large domain of the torque-speed plane. We will call this efficiency map as level-0 model for the e-drive as it gives an accurate calculation of the output power from the input power. This model is used in chapter 3 and chapter 4 to build the simulation of the global vehicle.
The component's models have the parameters derived and calculated according to data for Renault ZOE car. The electrical drive is modelled by a static model based on an efficiency map provided by RTR (Figure 10).

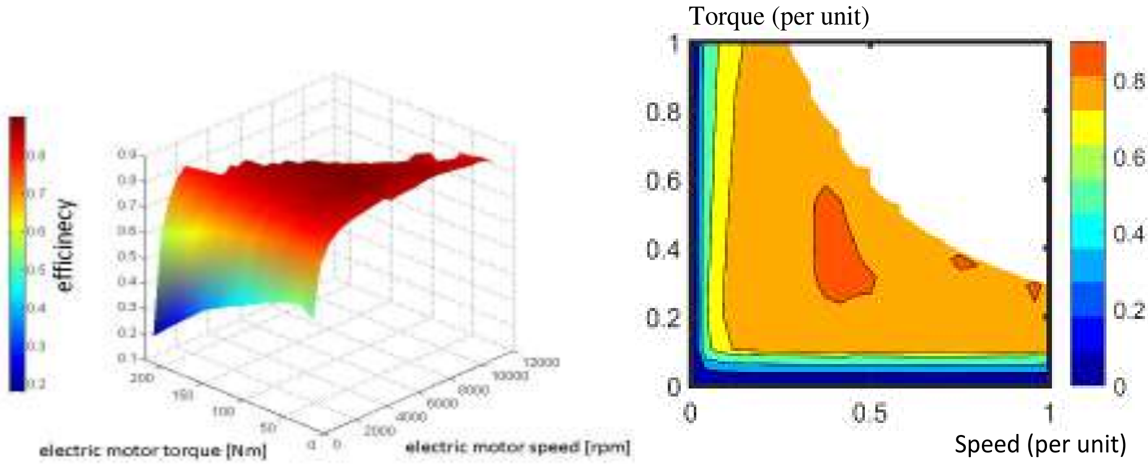

Figure 10 Efficiency map of the e-drive

The EMR representation (Figure 9) has been implemented in Matlab-Simulink© (Figure 11) thanks to the EMR library [EMRwebsite 2019]. The level-0 battery model described in the previous chapter and the level-0 e-drive model were linked with a gearbox model, wheel model and chassis model as described in Figure 9. The gearbox model, wheel model and chassis model compose the car body model. This is level-0 model of the BEV implemented in Matlab-Simulink©.

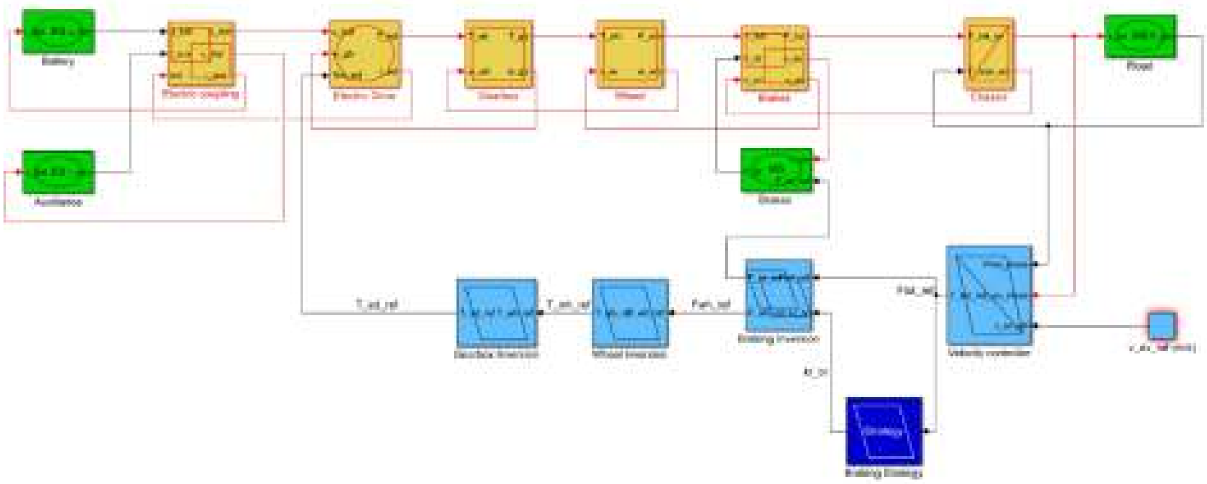

Figure 11 Matlab-Simulink© subsystems of the studied BEV

The validation of the developed model is done using data and measurements provided by RTR from a mixed urban and extra urban cycle. This driving cycle consists in a trip of 83 km for a duration of 1h 40 min (Figure 12). The initial SoC was 97% and the final SoC was 61.8%.

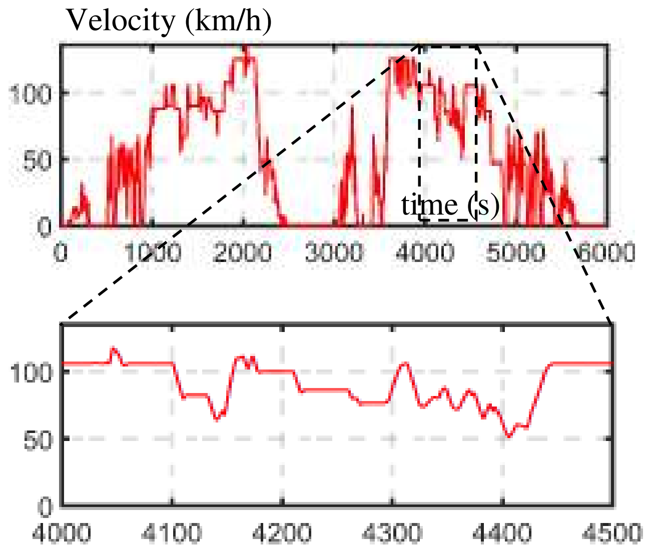

Figure 12 Studied driving cycle (velocity profile)

The measured velocity profile has been used as input for the simulation. A constant current was considered for auxiliary consumers. The value of the constant current considered is 0.6 A as observed in the real test. Both simulation and experimental results can now be compared.
For the battery current (Figure 13), the experimental current has more peaks than the simulation one. It can be explained by the static model of the e-drive where no dynamics are considered. Moreover, the inverter is indirectly considered by an average model instead of an instantaneous model: the effect of the modulation is thus neglected. Finally, the driving and operation conditions (slopes, weather, wind, regenerative braking strategy etc.) are not totally known. The average error of the rms current are about 15%. The accuracy could be improved by a dynamical model of the e-drive and more details on the driving and operation conditions.

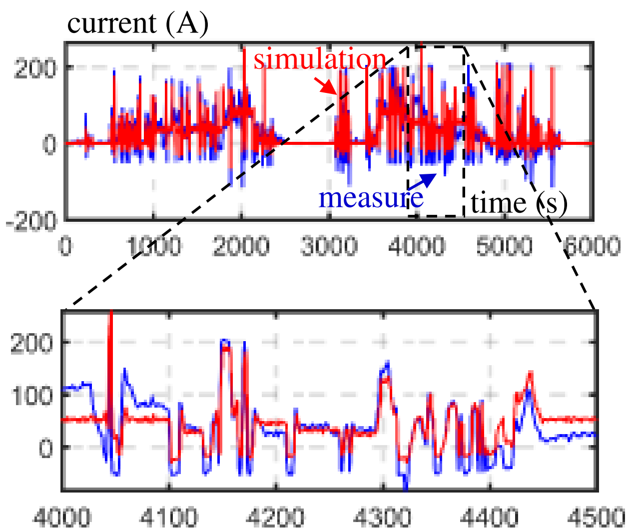

Figure 13 Current on the High Voltage Battery

The battery voltage (Figure 14) and SoC (Figure 15) are also compared. For these variables the error is lower because the battery acts as a filter. Both errors are about 1.3 %. We can deduce that the battery parameters are well identified. Of course, the ripples due to the converter modulation, and the measurement noise are not observed in the simulation results.

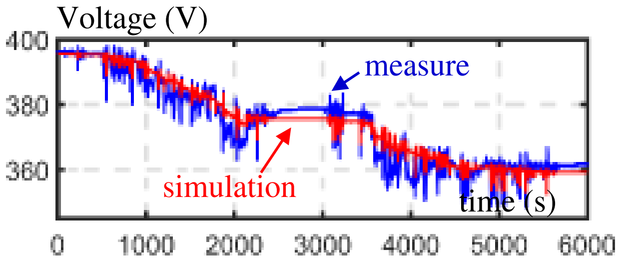

Figure 14 Voltage of the HV battery

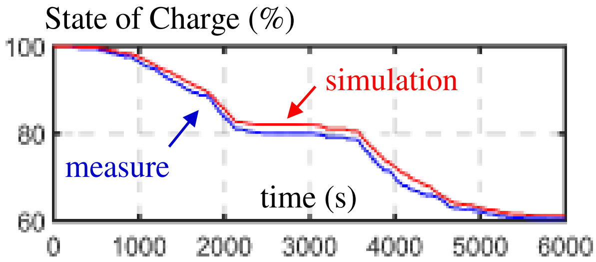

Figure 15 Battery State of Charge

The final energy consumption is 15.99 kWh for the measured trip and 15.64 kWh for the simulated trip. That leads to a difference of 2.20% that is acceptable at the vehicle level (Figure 16).

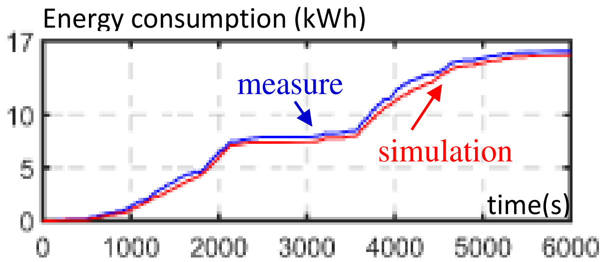

Figure 16 Battery's energy consumption

4. Simulation and validation of the studied BEV using Simcenter Amesim©

Simcenter Amesim© software has been extended by developing a dedicated library to apply the EMR methodology as presented in previous report [PANDA D4.1]. The EMR library has been designed to facilitate the development of new custom EMR simulations, by making the EMR components readily available such that work is not required in constructing them. This new library contains subsystems with pictograms and colours of EMR elements and enables the development of EMR vehicle models (and other EMR systems) within Simcenter Amesim© (Figure 17). The pictograms are in agreement with the EMR formalism from Table 2, so it is much easier to build simulations using these blocks. These blocks have the ability to be connected to other blocks in Simcenter Amesim© as it has compatible ports (fixed inputs and outputs).
To develop and run EMR simulations in Simcenter Amesim©, two libraries are used: the new developed EMR library (Figure 17) and the existing Signal & Control library to realize the model within each EMR block. Thus, all the models of systems are built using these elements and following the EMR rules. Signals treatment and simulation parameters are the same as for any Simcenter Amesim© simulation so a user of this software tool will have no problem to use the new developed library.

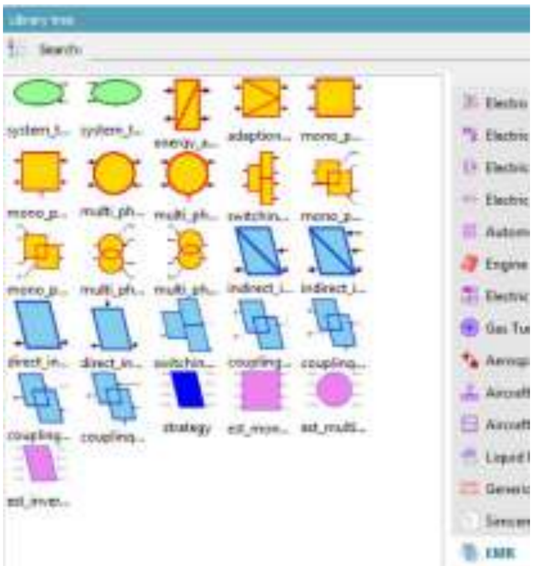

Figure 17 EMR library in Simcenter Amesim©

In order to build a similar simulation of studied BEV, Renault ZOE, the same equations (1)-(10) were implemented using EMR library in Simcenter Amesim© (Figure 17).
The description of level-0 BEV model implemented is in Figure 18:

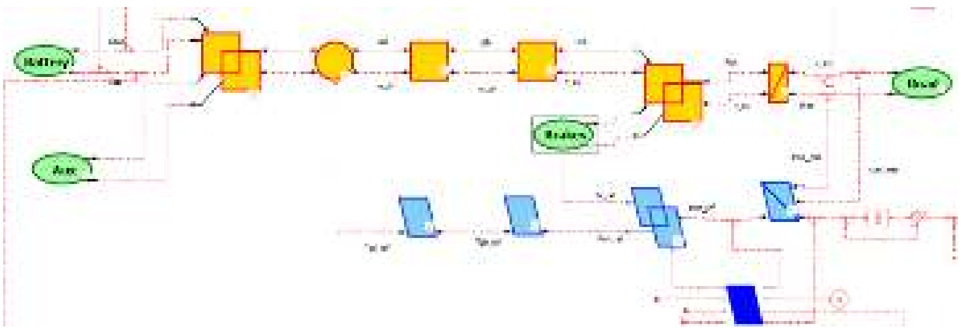

Figure 18 Simcenter Amesim© model of BEV Renault ZOE

It should be notice that the EMR-based simulation in Simcenter Amesim© is more in agreement with EMR rules than the one of Matlab-Simulink© (see Figure 11). This specificity is ensured thanks to the dedicated EMR library developed in PANDA for Simcenter Amesim©.

As results from this simulation, the same parameters from previous section were plotted in Figure 13. Here, we can compare the results from Matlab-Simulink© (from Figure 13 to Figure 16) with the results form Simcenter Amesim© simulation. The colours of signal plotted are inverted comparing to figures from Matlab-Simulink© simulation: now the simulation results are plotted in blue and measured variables are plotted in red to facilitate the difference. The difference from both simulations is very small and is done by different optimisation technics for numerical calculation used by the two software. As the model parameters are the same and the modelling equations implemented are the same, there is no reason to have visible differences in the two simulations.

The numerical results for total energy consumption from the battery were almost the same values in both simulation 15.99kWh and compared with the measured value of 15.64kWh gives the difference of 2.20%. This difference obtained on a mixed urban and extra urban cycle of about 1h 40min long is a very good value for such a simple model. The level-0 model of the e-drive was obtained from measurements on a bench so, during the vehicle development this precision in energy consumption calculation can be obtained before the vehicle assembly.

For a shorter test cycle, as standard cycles NEDC and WLTP, the precision of the energy consumption calculation is even better, so this model can be used in this case too.

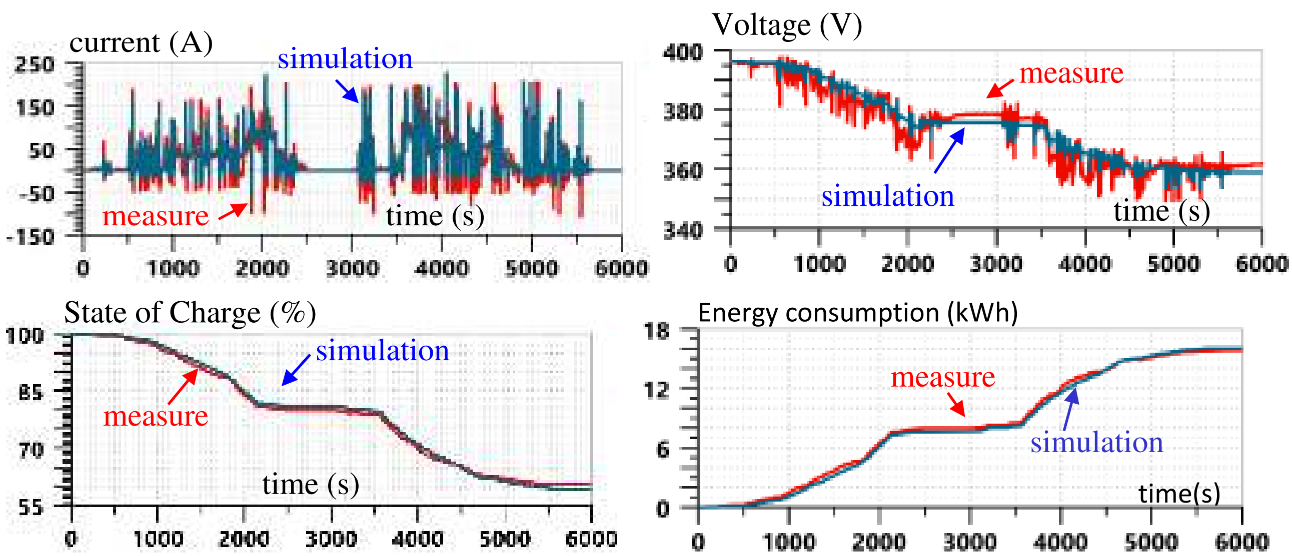

Figure 19 Simcenter Amesim© simulation results for the level-0 model of the BEV

5. Multi-level simulation of the studied BEV using Simcenter Amesim©

In this chapter, there are presented different models of subsystems of the studied BEV, Renault ZOE, as they were developed and the use of them for simulation of the vehicle. The models were developed using EMR formalism and validated in Matlab Simulink© software that is familiar for the developers of the models. Then the models were implemented in Simcenter Amesim© software and they were tested by comparing the experimental results with simulation results from Simcenter Amesim© using the same inputs and the same parameters. As the results are very close, they prove the straightforward implementation of the EMR formalism in different software tools.

In this section, we will test the interoperability of the simulation approach by using different model levels of subsystems for the studied BEV. If this multi-level simulations have been achieved on both software packages, only the results with Simcenter Amesim © are reported here. Indeed, this software is the selection of PANDA to capitalize the different models and also to develop the cloud of models.

5.1 Battery models

Battery models were developed in work package 2 (WP2) and the report [PANDA D2.1] presents the two battery models developed. In WP2 the two models of the battery used by Renault ZOE from actual tests were developed and validated with an NEDC test and a real test on Renault ZOE vehicle. They were validated in EMR representation. The models are implemented in Matlab-Simulink© and Simcenter Amesim© following EMR rules as they are described in following paragraphs.

A level-0 battery model was introduced in Chapter 2 by equation (1). Next paragraphs present more detailed battery models.

5.1.1 Level-1 battery model

The considered level-1 battery model is a pure electrical model of a cell multiplied by the number of cells of the real battery. It is respected the connection architecture of the cells and packs in the real battery.

The electrical model of a cell is built on the 1st order Thevenin model [Huria 2012] (Figure 20) and consists in a voltage source with an ohmic resistance and a parallel RC circuit. Based on the equivalent circuit model, the cell output voltage of the Li-ion cell is the voltage drop resulting from the battery open-circuit voltage (OCV), the battery ohmic resistance (R_0), and battery polarization impedance (R_1C_1 circuit).

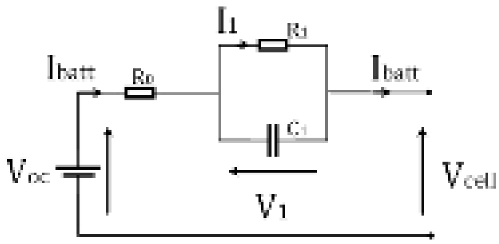

Figure 20 Representation of the 1st-order Thevenin model

The Renault ZOE battery level-1 model in EMR implemented in Simcenter-Amesim© is presented in Figure 21[1]. The cells are arranged in packs and connected according to real battery connections (n_s number of cells in series in a branch, and n_p number of branches in parallel in the pack). To obtain the battery pack voltage, the voltage of one cell is multiplied by the number of series connections. All cells are assumed to be identical that enables to use an adaptation element in the EMR formalism (see equation 13 and 14).

$$u_{Cell} = OCV_{Cell}(SoC) + R_{bat}i_{Cell} \tag{13}$$

[1] If all modelling equations can be implemented in a single oval pictogram, we prefer to propose here a detailed EMR of this model for better understanding and also for a differentiation with the level-0 model.

$$\begin{cases} u_{bat} = n_s u_{Cell} \\ i_{Cell} = n_p i_{bat} \end{cases} \quad (14)$$

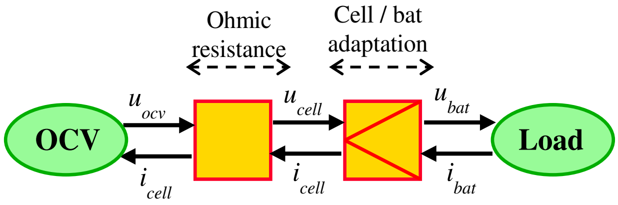

Figure 21 EMR representation of the Renault battery model

The corresponding model of the level-1 battery model in Simcenter Amesim© using EMR library developed is presented in Figure 22. As one can notice, the input and output ports are the same signals: the battery current is input and the battery voltage and the State Of Charge (SOC) are output variables.

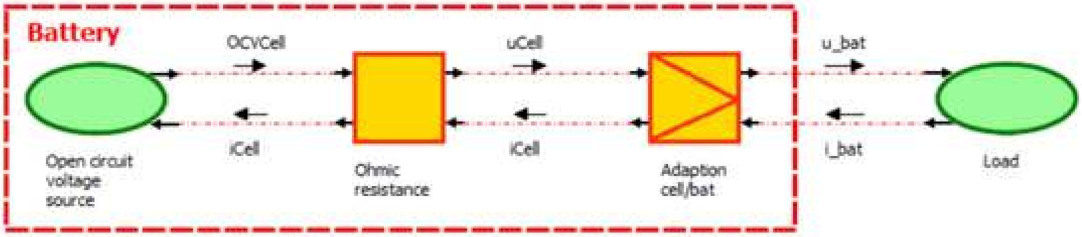

Figure 22 Simcenter Amesim© block used for level-1 battery model for global vehicle simulation

5.1.2 Level-2 battery model

The level-2 battery model is an electro-thermal model [Jaguemont 2015] [German 2020]. The electrical part of the model is the level-1 battery model and is presented in the previous subsection. Concerning the thermal model, the battery pack is considered as a single thermal component with one temperature point. This means a global heat generation, specific heat capacity and convective coefficient are considered, only the mass is multiplied by the total number of cells, assuming that Joule losses are equally generated from all cells [PANDA D2.1]. The electro-thermal model of one cell in EMR representation is presented in Figure 23 (all modelling equations can be found in [PANDA 2.1]). The description of the parameters and variables from Figure 23 is in Table 3.

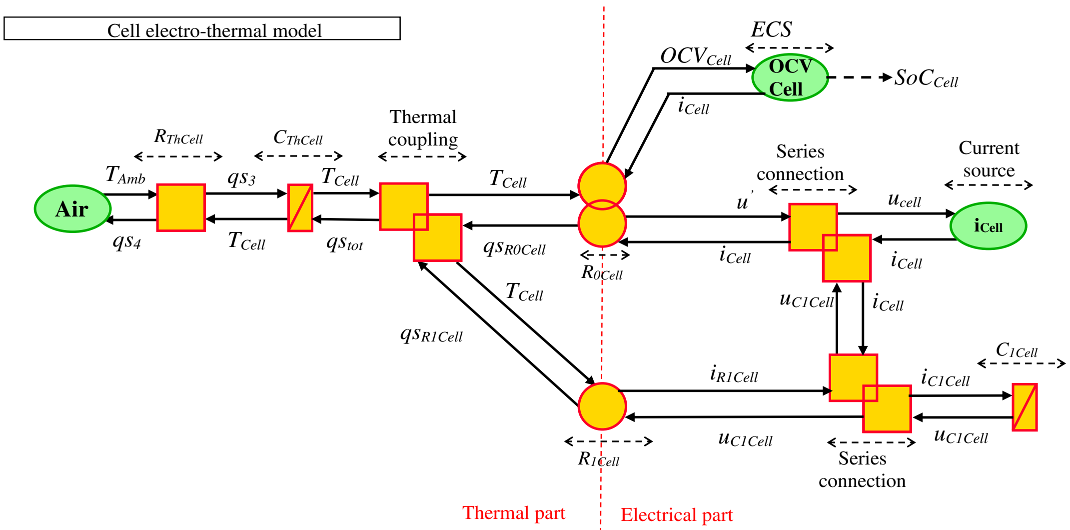

Figure 23 EMR representation of the dynamical electro-thermal model for a single cell

Table 3 List of parameters and variables

	Symbol	Description	Unit
Electrical part	C_{AhCell}	Cell capacity	A.h
	R_{0Cell}	Cell series resistance	Ω
	R_{1Cell}	Cell diffusion resistance	
	C_{1Cell}	Cell diffusion capacitance	F
	SoC_{Cell}	Cell state of charge	%
	OCV_{Cell}	Cell open circuit voltage	V
	u'_{Cell}	Cell internal voltage after R_{0Cell} drop	
	u_{C1Cell}	Cell voltage drop due to R_{1Cell}//C_{1Cell}	
	u_{Cell}	Cell voltage at the terminals (+/-)	A
	i_{Cell}	Cell current through the terminals (+/-)	
	i_{R1Cell}	Current though R_{1Cell}	
	i_{C1Cell}	Current though C_{1Cell}	
Thermal part	C_{ThCell}	Cell thermal capacitance	$J.K^{-1}$
	R_{ThCell}	Cell thermal resistance	$K.W^{-1}$
	T_{Cell}	Temperature inside the cell	K
	T_{Amb}	Temperature of the ambient air surrounding the cell	
	$q_{SR0Cell}$	Cell heating entropy flow due to Joule effect in R_{0Cell}	$W.K^{-1}$
	$q_{SR1Cell}$	Cell heating flow due to R_{1Cell}	
	$q_{STotCell}$	Cell heating entropy flow due to *global Joule effect*	
	q_{S3}	Cell cooling entropy flow (from the inside of the cell to the surface)	
	q_{S4}	Cell cooling entropy flow (from the surface of the cell to the ambient air)	

To build the model of the entire battery pack the connection of series and parallel cells from real battery of the BEV was respected. The corresponding description of the level-2 battery model in Simcenter Amesim© using EMR library developed is presented in Figure 24.

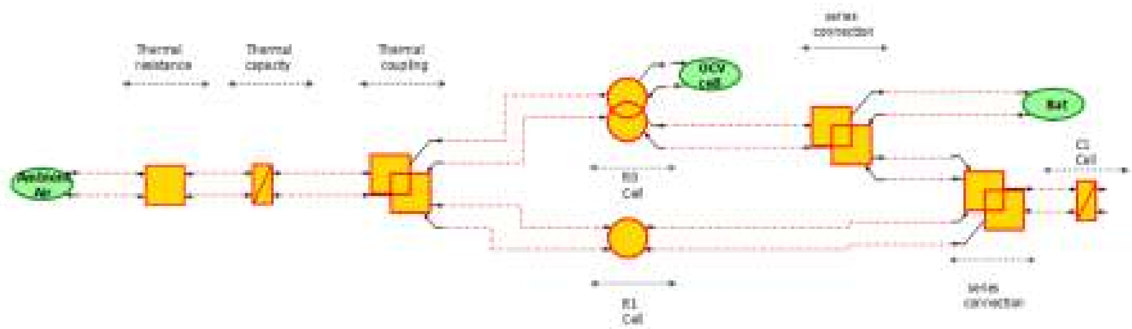

Figure 24 Simcenter Amesim© block diagram for level-2 battery model

5.2 Electric drive (e-drive) models

The electric drive (e-drive) models of Permanent Magnet Synchronous Motor (PMSM) were developed in work package 3 (WP3) and presented in [PANDA D3.1]. PMSM is the most used electrical machine in e-drives for electrical and hybrid vehicles. It is compact and have a high efficiency. There were developed 3 models for 3 levels of detail of PMSM. The models were implemented in Matlab-Simulink© and in Simcenter Amesim© simulation tool using EMR method. They were validate using a test bench for a PMSM. The actual report refers to the validation of e-drives for the specific BEV studied in PANDA project, Renault ZOE. This vehicle has a different electric motor than other BEVs, a Wound Rotor Synchronous Machine (WRSM). This motor is similar with PMSM, but the magnetic field produced by the rotor doesn't come from permanent magnets, it is produced by a coil on the rotor and it is fed by a separate DC circuit. This type of electric motor is a little bit bigger than PMSM because it must contain the coil on the rotor (which is a bigger than permanent magnets) and also a rotating connector for the coil on the rotor. It needs a separate current

controller for the rotor coil current to provide a variable magnetic field. This variable magnetic field gives this motor an advantage in terms of flexibility – it can work with high efficiency in larger limits of torque and speed. The control strategy and the model of the stator is similar with the one applied to PMSM.
The WRSM models was not presented in the previous report so they are shortly described in the following paragraphs. They were implemented Matlab-Simulink© and Simcenter Amesim©. The validation of these models was done using vehicle tests.

5.2.1 Level-1 e-drive model

The first Wound Rotor Synchronous Machine (WRSM) model uses constant parameters (e.g. L_d, L_q, L_f, M_f) [Raia 2019]. Hence it doesn't take into consideration the saturation, nor the cross-saturation effects. The machine is modelled as an inductive-resistive load, while the transformation of electrical energy to mechanical energy is characterized by the torque equation. The *dq*-currents are directly obtained from the voltage equation [Boldea 2005].
The mathematical model of the wound rotor synchronous machine under study in *dq* reference frame is described by the following equation:

$$\begin{bmatrix} v_d \\ v_q \\ v_f \end{bmatrix} = \begin{bmatrix} R_s & 0 & 0 \\ 0 & R_s & 0 \\ 0 & 0 & R_f \end{bmatrix} \begin{bmatrix} i_d \\ i_q \\ i_f \end{bmatrix} + \begin{bmatrix} L_d + M_f & 0 & M_f \\ 0 & L_q & 0 \\ M_f & 0 & L_f + M_f \end{bmatrix} \frac{d}{dt} \begin{bmatrix} i_d \\ i_q \\ i_f \end{bmatrix} + \begin{bmatrix} e_d \\ e_q \\ e_f \end{bmatrix} \tag{15}$$

Where v_d, v_q, are stator voltages and i_d, i_q are stator currents expressed in *dq* reference. The stator parameters R_s, the resistance and L_d, L_q stator inductance are also expressed in *dq* reference and M_f is the mutual inductance between the rotor and each stator inductance. All these parameters are constant. The rotor parameters R_f, the resistance and L_f the inductance are also constant, while v_f and i_f are the voltage and the current of the rotor field. The electromotive forces (back-emf) in the stator circuits, e_d and e_q, and e_f for the rotor circuit are also present in equation (15).
The energy conversion is obtained in the WRSM block, the resulting electromagnetic torque from the stator fluxes Ψd and Ψq, stator currents i_d, i_q , and number of pole pairs p:

$$T = p(\psi_d i_q - \psi_q i_d) \tag{16}$$

The e-drive level-1 model of the assembly converters-electric motor using the EMR formalism is presented in Figure 25. The converters are described by mono-physical energy conversions, voltage sources (u_{abc},u_f).

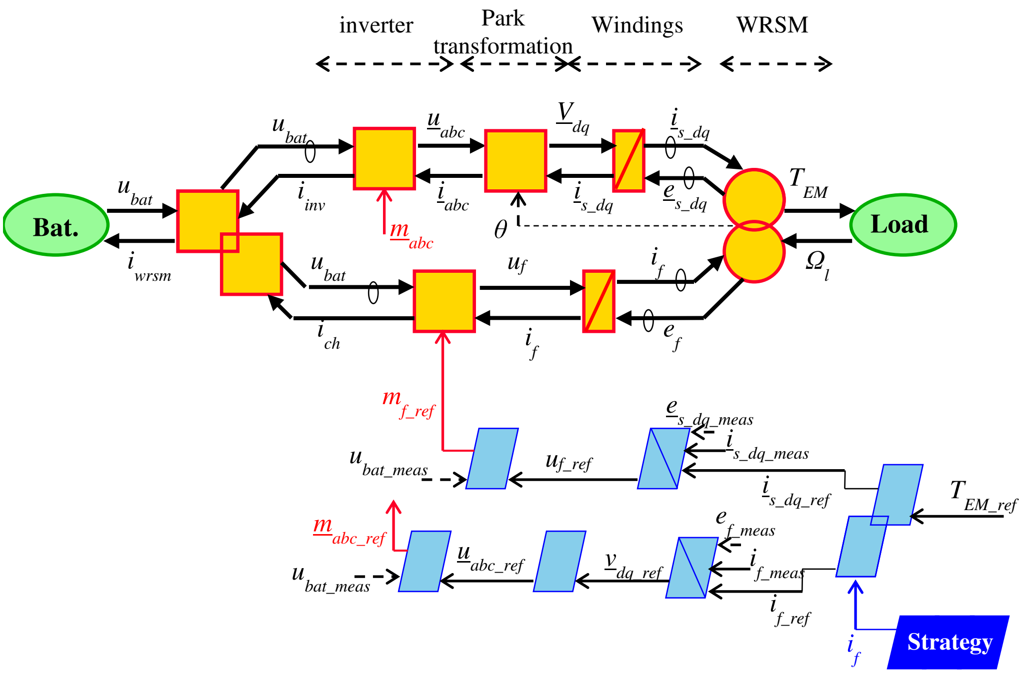

Figure 25 EMR representation of the level-1 model of the e-drive

The e-drive model integrates the electrical machine, a simplified model of the voltage source inverter (VSI) and the control unit, based on an indirect field-oriented control (FOC). The model was also implemented in Simcenter Amesim© using the developed EMR library and it was tuned with data for the e-drive from the studied BEV. The implementation of this model is presented in Figure 26.

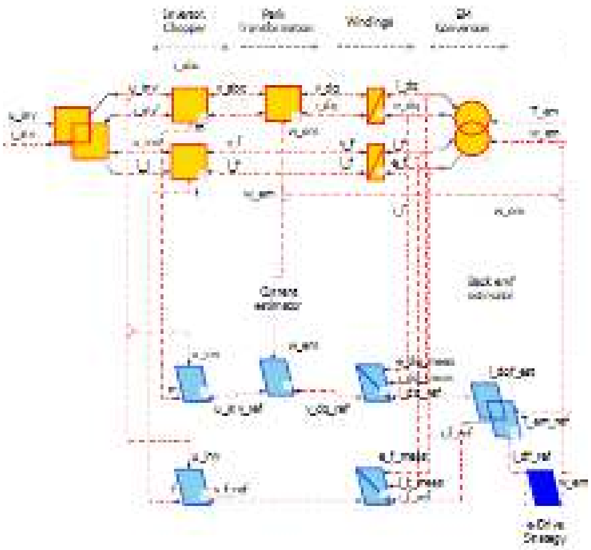

Figure 26 Simcenter Amesim© block diagram for level-1 e-drive model

5.2.2 Level-2 e-drive model

The second wound rotor synchronous machine model is created using constant parameters and uses as variables, besides the *dq*- and excitation currents, the flux linkages. The mathematical model of the wound rotor synchronous machine under study in *dq* reference frame is described by the voltage equations, the relationships between currents and flux linkage values and torque equation [Szabo 2009].
In the stator winding block, the flux linkage values are obtained from the voltage equation. After that, the i_d, i_q and i_f currents are obtained by solving the following system of equations (17):

$$\begin{gathered}\psi_d = L_d i_d + M_f(i_d + i_f) \\ \psi_q = L_q i_q \\ \psi_f = L_f i_f + M_f(i_d + i_f)\end{gathered} \tag{17}$$

Once the i_d, i_q and i_f currents are obtained, the energy conversion is performed in the WRSM block.
As in the previous model, the e-drive model integrates the electrical machine, a simplified model of the voltage source inverter (VSI) and the control unit, based on an indirect field-oriented control (FOC). Besides this, two estimation blocks are introduced (for the *dq* frame currents and back-emfs) in order to implement the control strategy. The back-emf values that result from the estimation block are given by the following equations (18):

$$\begin{gathered}e_d = -\omega\psi_q \\ e_q = \omega\psi_d\end{gathered} \tag{18}$$

The e-drive level-2 model using the EMR formalism is presented in Figure 27 [Baert 2012] [Ruba 2019]. The same as for previous model, the converters are modelled as mono-physical energy conversions, voltage sources (u_{abc}, u_f). It should be noted that the estimation blocks (purples elements) have been added to provide the estimation of non-measured variables, as in the real implementation of a field-oriented control. Thus, the e-drive level-2 model is closer to the real system offering more information.

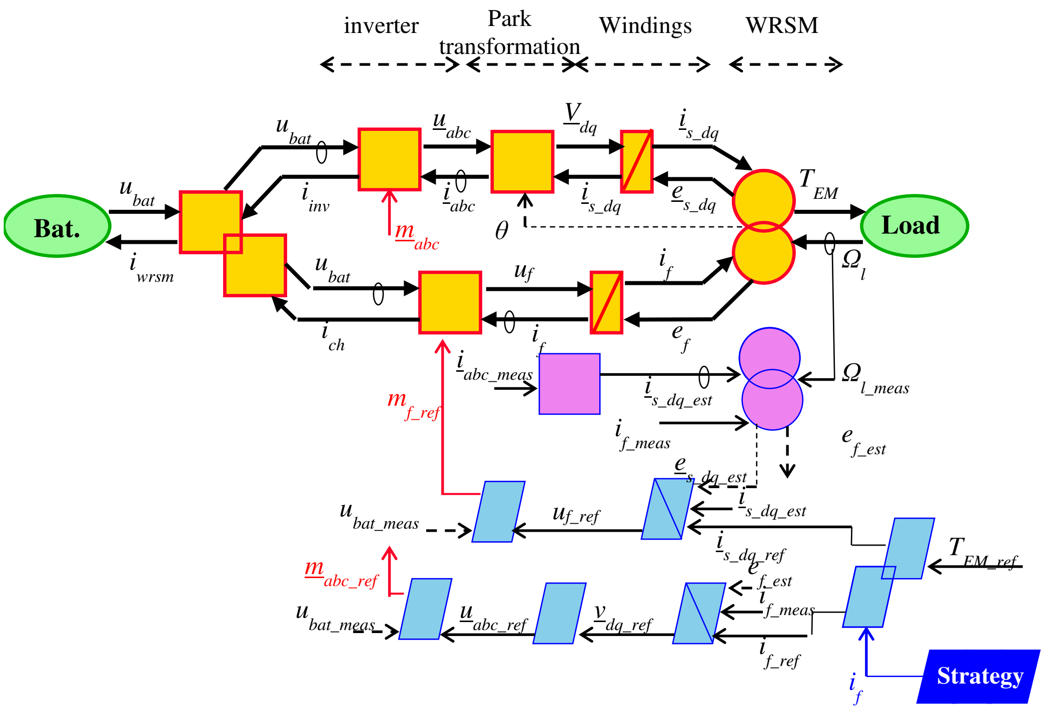

Figure 27 EMR representation of the level-2 model of the e-drive

For implementation in Simcenter Amesim©, a simplified model of the voltage source inverter (VSI) and chopper was chosen. The model was tuned with data for the e-drive from the studied BEV, Renault ZOE. Then the model was implemented with the same parameters using the developed EMR library. The description of this model is presented in Figure 28. The model was tested and validated using measurements just like it was done for the previous model.

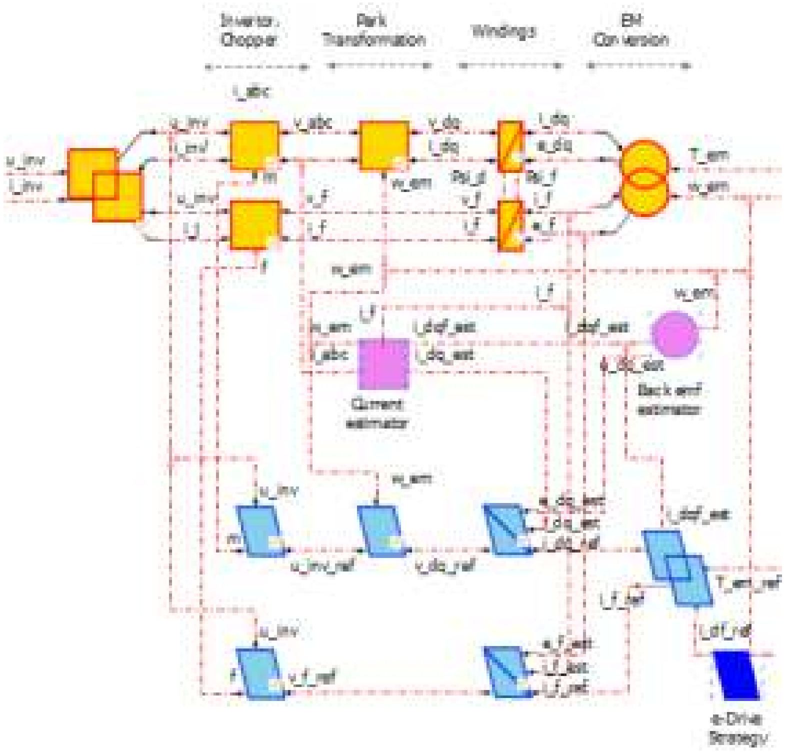

Figure 28 Simcenter Amesim© block diagram for level-2 e-drive model of the BEV

5.3 Car body model

In this report, it is proposed to use only one car body model for all simulations. As the purpose of the simulations is to calculate energetic performances of the car, the car body is just a transformation for all resistance forces to the torque on the shaft of the electric motor. Equations for the car body remains the same as there were presented in section 2, equation (4)-(10). So the EMR representation of the car body can be identified in Figure 9 and it is presented detailed in Figure 29

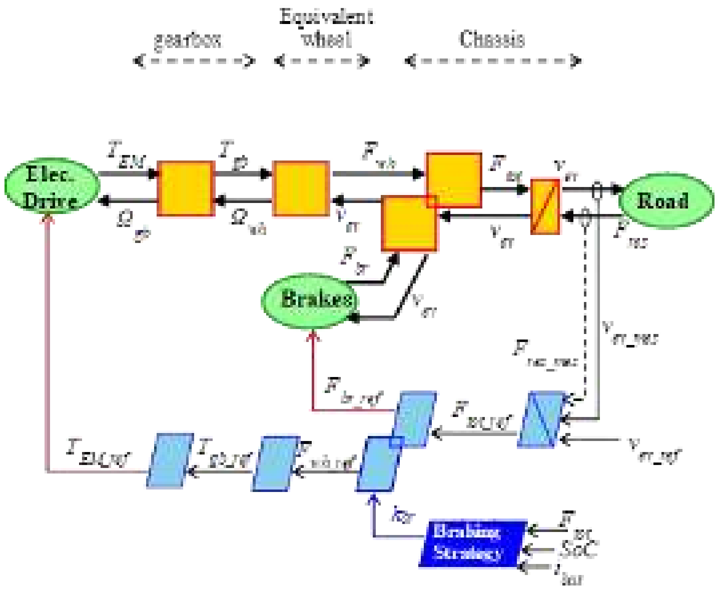

Figure 29 EMR representation of the car body

It is taken into account in this model all the transformations needed by the control of the e-drive to obtain the “load” torque on the electrical machine shaft, $T_{\_em\_ref}$ (Figure 30 Figure 29– blue blocks). This group of blue blocks it is named in Figure 31 as Body Control.

Using EMR library developed, the car body model was implemented in Simcenter Amesim© and the picture of the model is presented in Figure 30.

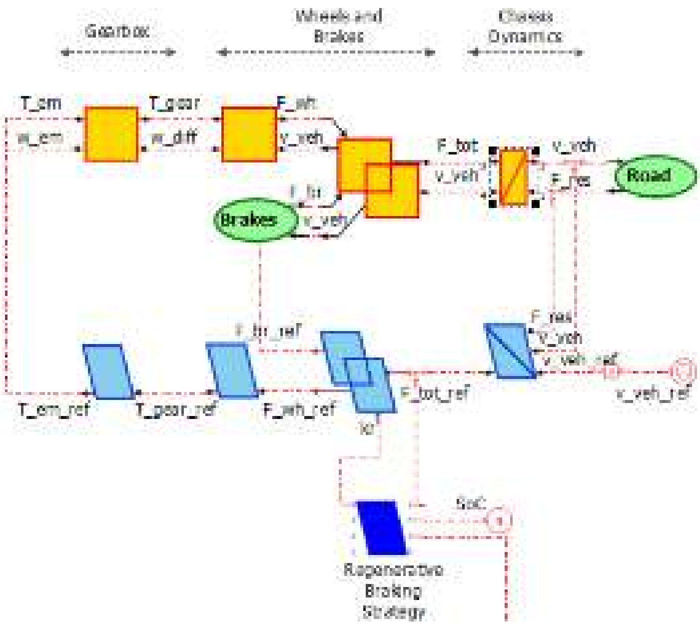

Figure 30 Car body model in Simcenter Amesim©

5.4 Multi-level simulation of the studied BEV validated on different test scenarios

This subsection presents the results of simulation of multi-level models of the studied BEV, Renault ZOE compared with experimental results provided by RTR according to agreed test scenarios. First test is a highway driving cycle where the car runs with slow speed variation between 100 km/h and 130km/h, without stopping during the test. For a BEV, it is a high energy consumption test where all subsystems are working close to their limits. However, as the car speed is high the cooling systems are working well and all subsystems are not reaching their thermal limits. During the test, there are no derating in performances of the subsystems. In the Renault ZOE car, the battery is air cooled and the cooling is efficient and constant during this test. As the energy consumption is high, the battery discharge rapidly and almost at constant rate and one can validate the SoC model by comparing with real SoC measured. The SoC is an important variable because it is directly related to the autonomy of the BEV, a very sensitive requirement for customers of a BEV and BEV benchmark attribute.

There are simulated different model configurations of the BEV, Renault ZOE, in order to prove the flexibility of the model organisation as they can be replaced quickly on the simulation architecture because the EMR impose the same connection ports and the same internal structure of the models. This organisation ensures the compatibility of the connected models and there are no simulation errors when models are changed. From Figure 31, every block, which represents a subsystem model, can be replaced by another model with a different level of details. They can be quickly connected in the global simulation due to standard input and output ports.

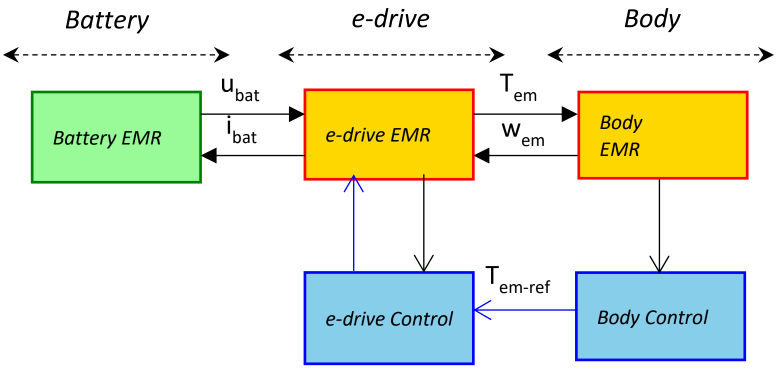

Figure 31 Structural architecture of BEV simulation

Different models of battery and e-drive are connected to the same car body model as it is important to compare the performances of the different models used in the global vehicle simulation. As it is mentioned above, the SoC is an important variable and together with energy consumed from the battery, they give the efficiency and the autonomy of the BEV, the most important variables for the vehicle.

The models implemented in Simcenter Amesim© are connected according to the structure from Figure 31 following the EMR rules [Husar 2019]. The next paragraphs present the results of simulations compared with the measurements. There are parts of the cycle where the simulated variables are very close to the measured ones and there are parts where there are differences. These differences are due to the unknown test conditions as the test was done on a real highway with different rolling surfaces, wind change conditions, slow slopes and pressure variation because of traffic conditions. These uncertainties can't be modelled but the global energy consumption must be calculated close to the real energy consumption for a good simulation.

For all the comparisons at the vehicle level, it should be reminded that all measurements have uncertainties due to the sensor accuracy and also to measurement noise. For this reason, any simulation results within +/- 2% of errors compared with the experimental results, will be considered as acceptable. Any variation within this 2% range will be not considered as significant.

5.4.1. Simulation of level-1 configuration model for the highway test scenario

The architecture of the simulation in this case is based on level-1 battery model presented in § 5.1.1 connected to level-1 e-drive model presented in § 5.2.1 also connected to car body model presented in § 5.3. This architecture is implemented in Simcenter Amesim© software using the developed EMR library. In Figure 32, there is the description of the global BEV. It can be noticed the level-1 battery model and level-1 e-drive model can be easily connected to the car body model. The parameters of these models are the same with the parameters of the models validated individually.
The first input variable for the BEV simulation is the total resistive force estimated from vehicle characteristics: rolling frictions, internal frictions and aerodynamic force. The other input variable is the vehicle speed profile as speed reference for the simulation – which was the measured speed of the vehicle.

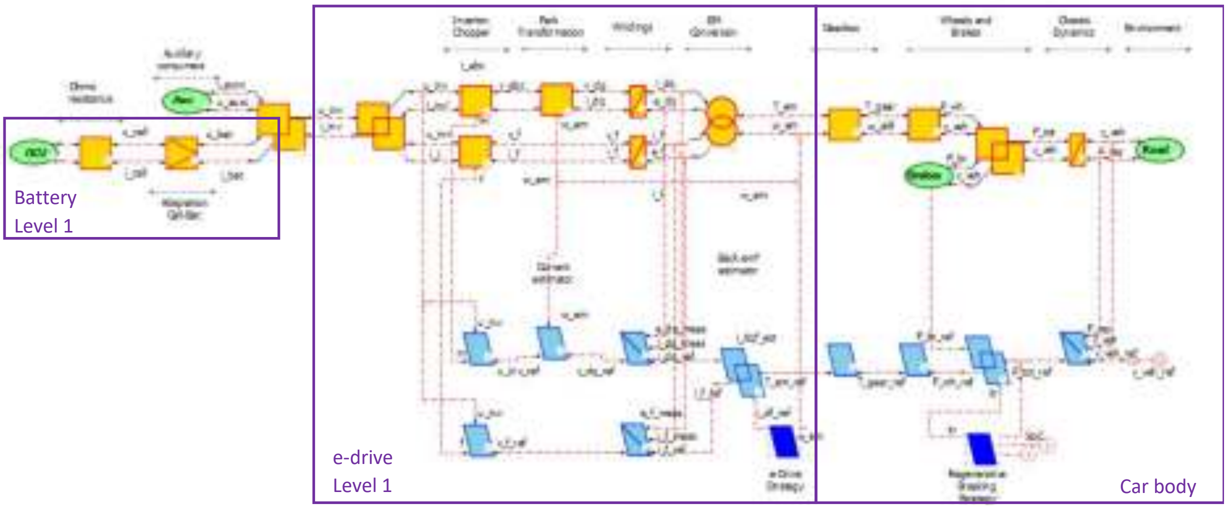

Figure 32 Level-1 model for BEV (level-1 models for battery and e-drive)

These variables are standard for energy consumption tests and simulations. For standard tests as NEDC or WLTP there are the standard speed profiles. During these standard tests, the time isn't long enough to evaluate the discharge of the battery so longer tests were preferred for validation of the proposed simulation architectures.
The total time of the simulation was the total time of the test, 4164 seconds (almost 1h:10min).
Table 4 shows the simulated variables and corresponding measured variables for the highway simulation. The pictures on the left column are for the whole simulation time and the pictures on the right column present a zoom for 200 seconds from the total simulation time.
Watching the detailed graphics on the right column it can be noticed some differences between simulation and measured signals for electric motor torque values and battery current values, especially during low rate variation of these parameters. These differences are due to environment uncertainties for test conditions mentioned above - different rolling surfaces, wind change conditions, slow slopes and air pressure variation because of traffic conditions.
For the evaluation of the precision of the simulation we are going to analyse the differences between simulation results and measured values for subsystem variables, the battery voltage and the battery current and for global variables, total energy consumed and state of charge of the battery. These global variables represent the target of such simulation as they give the efficiency of the vehicle and the autonomy of the vehicle.

Table 4 Comparison of level-1 simulated and measured parameters for the highway test

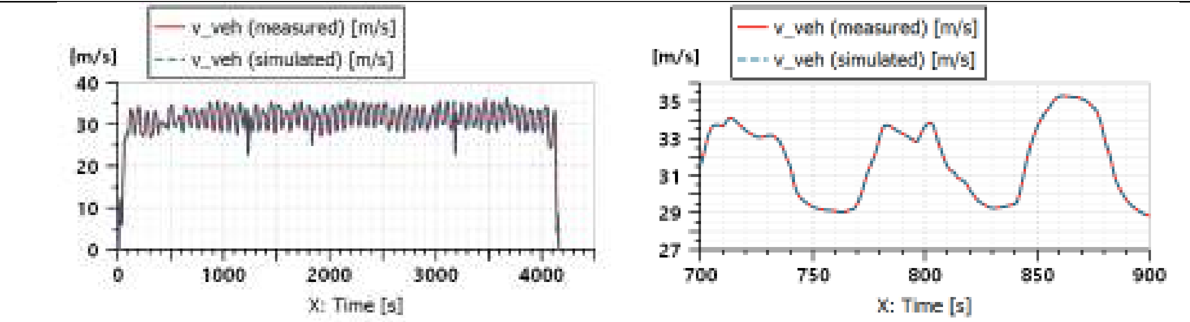

Vehicle speed

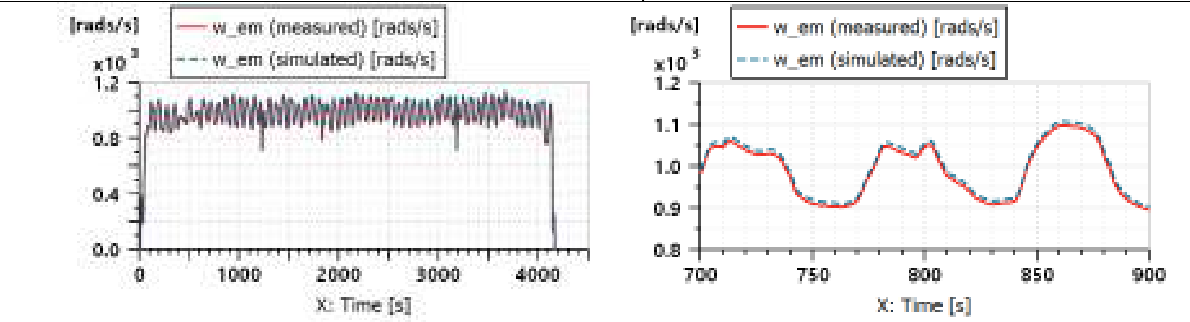

Electric motor speed

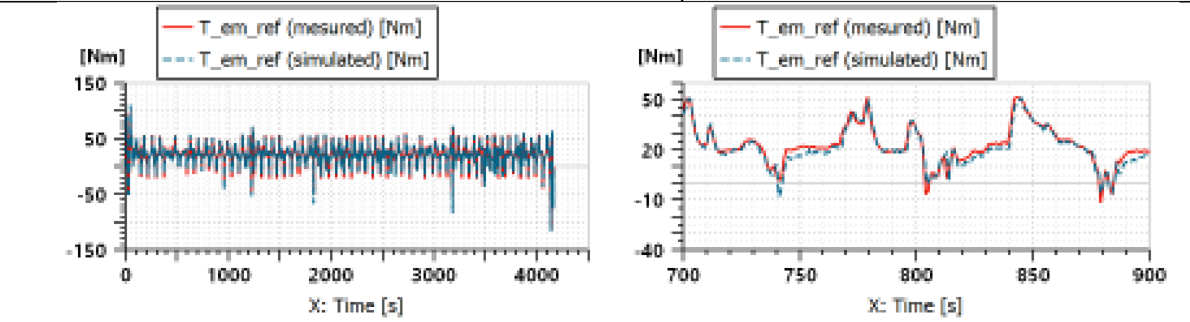

Electromagnetic torque

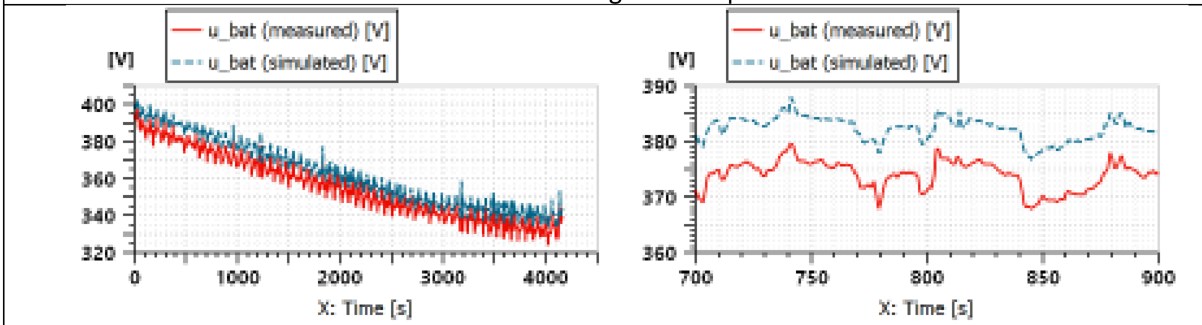

Battery voltage

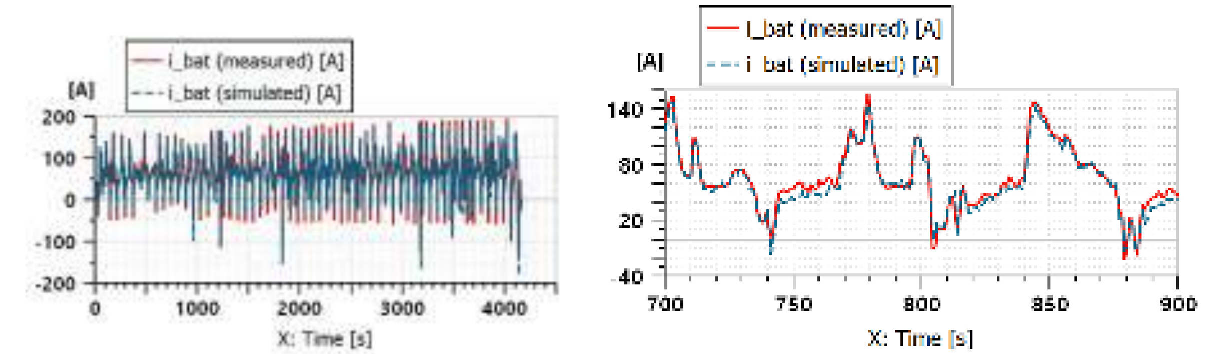

Battery current

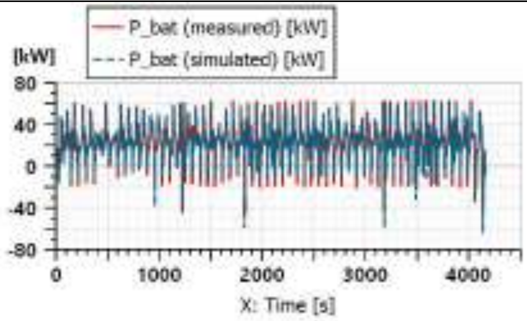

Battery power consumption

For the battery voltage, watching in Table 4 on the left column, the maximum difference between the filtered values of simulated and measured signal on the entire interval of the test is 8.47V. If we divide this difference to the average value of the measured voltage during all test of 357.3V we found the error of the simulated voltage of 2.3% on whole interval. For the zoom window of 200s from the picture on right column we have the difference of 8.3V which divided to the average value of 375.9V gives the error of the simulated voltage of 2.2% on the specified interval.
For the battery current the error is calculated related to the rms value of the signal on the whole interval using the formula form the equation (19):

$$errRMS(i\_bat) = \frac{|RMS(i\_bat_{meas}) - RMS(i\_bat_{sim})|}{RMS(i\_bat_{meas})} \cdot 100 = \frac{|83.50 - 79.26|}{83.50} = 5.77\ \% \qquad (19)$$

And for the zoom window of 200s of the battery current on the right column, the error is 4.82%
These errors for voltage and current (local variables) are quite low and shows a good correlation for variables of a subsystem of the car. More detailed models should reduce these errors.
For the global variables, the energy consumed from the battery and the state of charge of the battery (SoC) are compared with measurements in Figure 33. Both signals are almost linear because of the low highway speed variations. The final value of the graphic represents the total energy consumption during this test and the SoC of the battery at the end of the test.

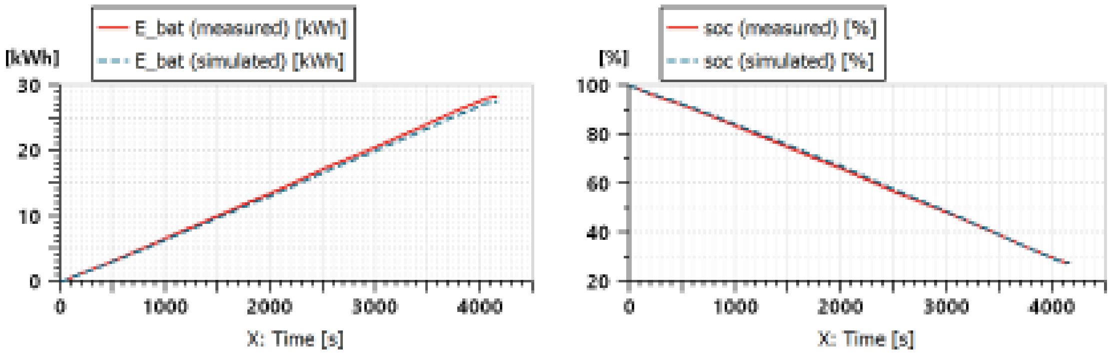

Figure 33 Energy consumption and SOC from simulation and test

By comparing with the measured value with the value obtained from simulation, it can be defined the error for the total energy consumption and the SoC error. For this test, the values of errors are given in equations (20). These low errors prove that the models developed and simulation architecture used give very accurate simulation results.

$$nerr(E_{bat}) = \left|\frac{E_{bat,meas} - E_{bat,sim}}{E_{bat,meas}}\right| \cdot 100\% = 2.55\%$$
$$err(SOC) = |SOC_{meas} - SOC_{sim}| = 0.1\% \qquad (20)$$

5.4.2. Simulation of level-2 configuration model for the highway test scenario

Following the architecture of the simulation, this case is based on level-2 battery model presented in § 5.1.2 connected to level-2 e-drive model presented in § 5.2.2 also connected to car body model presented in § 5.3. This architecture is implemented in Simcenter Amesim© software using the developed EMR library. In Figure 34 there is the description of the global BEV.

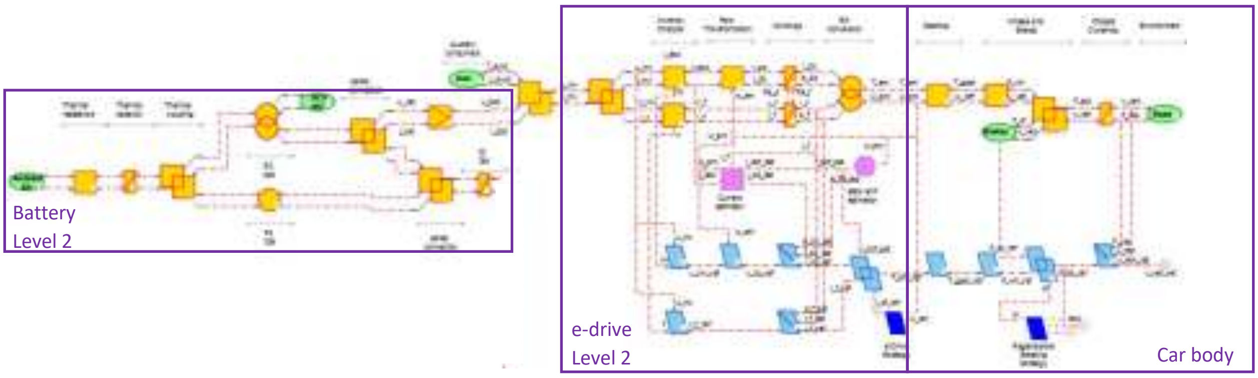

Figure 34 Level-2 model for BEV (level-2 models for battery and e-drive)

The same highway test of 1h 10 min was simulated using the new models on the same architecture. The results from the simulation are compared with corresponded measurements (Table 5). The pictures on the left column present the plots of the variables for the total simulation time and the pictures on the right column present the same zoom on 200s as it was presented in Table 4. Thus, there can be observed the performances of simulations regarding the same measurements. As expected, the simulated variables are also very close to the measurements and the differences that can be noticed for the current and torque simulation have the same cause, the environment uncertainties. The car body model and load model are not changed as the purpose of this simulation is to validate the flexibility of the model organisation proposed in the PANDA project. For the battery, this level-2 model provides internal temperature and this variable is also compared with values form the measurements (see Figure 36).

As for the previous simulation the evaluation of the precision of level-2 BEV model there are evaluated the battery current and battery voltage as subsystem variables and total energy consumed and SoC as global variables. The same error calculation is applied on the battery voltage and battery current signals for entire period of the test and for the zoom window of 200s from the right column.

All signals are presented in Table 5.

Table 5 Comparison of level-2 simulated and measured parameters for the highway test

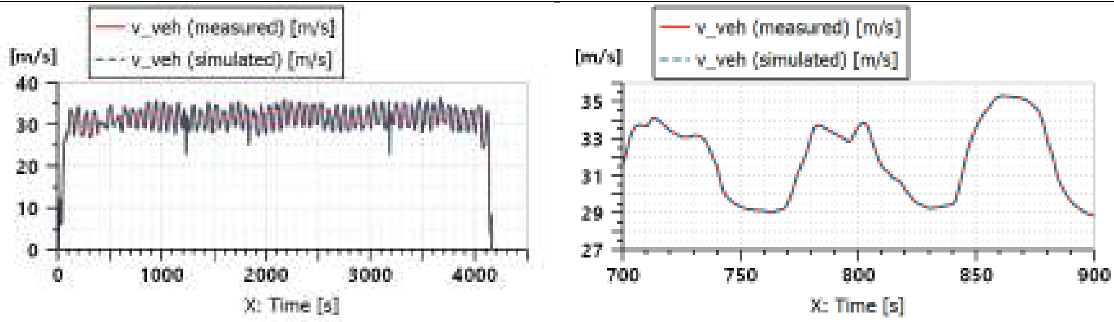

Vehicle speed

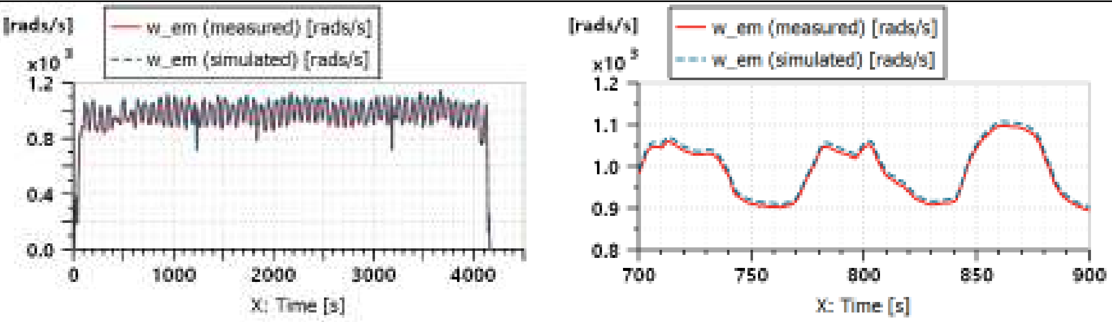

Electric motor speed

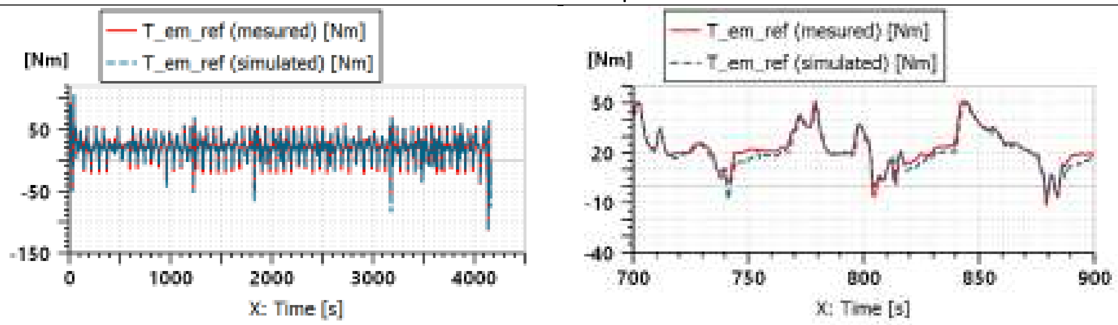

Electromagnetic torque

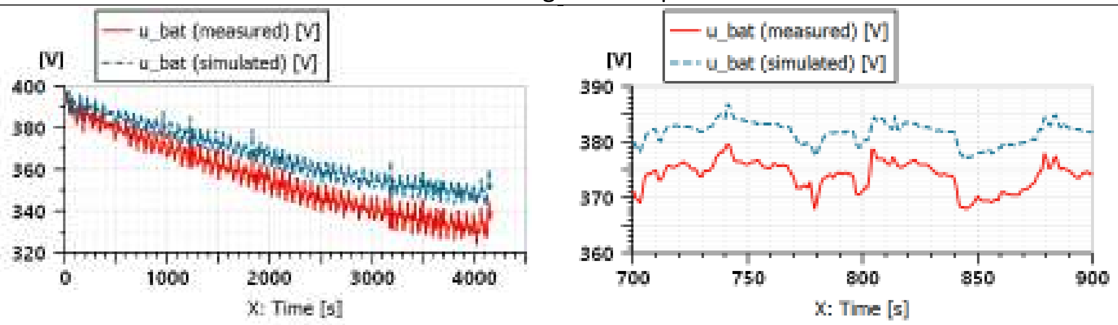

Battery voltage

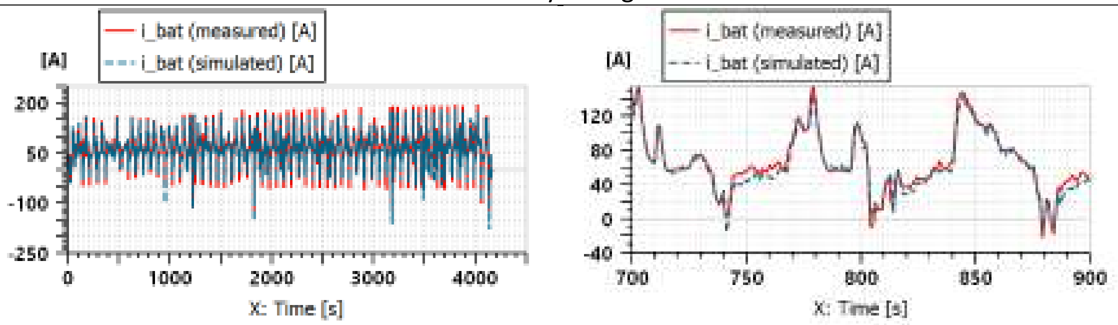

Battery current

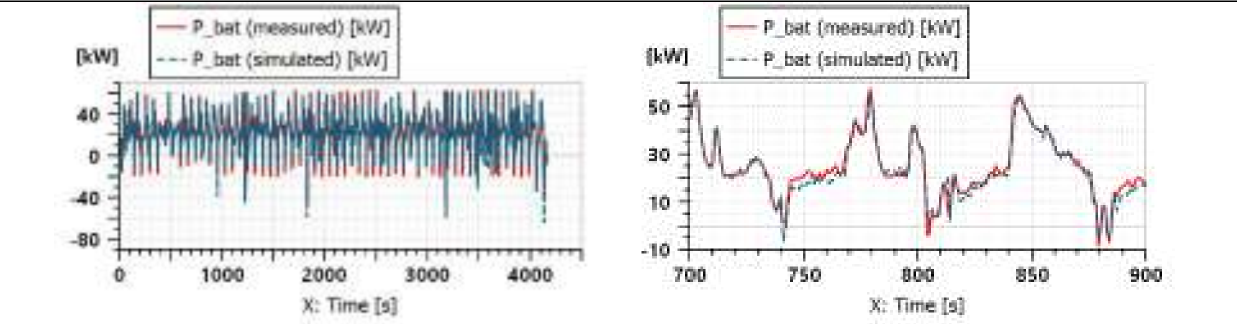

Battery power consumption

For the battery voltage signal on the left column, the maximum difference between the filtered values of simulated and measured signal on the entire interval of the test is 16.16V. This value divided to the average value of the measured voltage during all period of the test of 357.3V gives the error of the simulated voltage of 4.5% for level-2 model. For the zoom window of 200s from the picture on right column we have the difference of 7.28V which divided to the average value of 375.9V on that period gives the error of the simulated voltage of 1.9%
Similar with level-1 model analysis the battery current the error is calculated related to the rms value of the signal on the whole period of the test using the formula form the equation (21):

$$errRMS(i\_bat) = \frac{|RMS(i\_bat_{meas}) - RMS(i\_bat_{sim})|}{RMS(i\_bat_{meas})} \cdot 100 = \frac{|83.50 - 78.64|}{83.50} = 5.82\ \% \qquad (21)$$

For zoom window of the battery current of 200s the error of rms value is 4.08%. These error values are very close to the error values obtained for the simulation of level-1 models.
As there was done for the level-1 models, the energy consumption and the SoC of the battery are compared with the measured values for this level-2 global model in Figure 35.

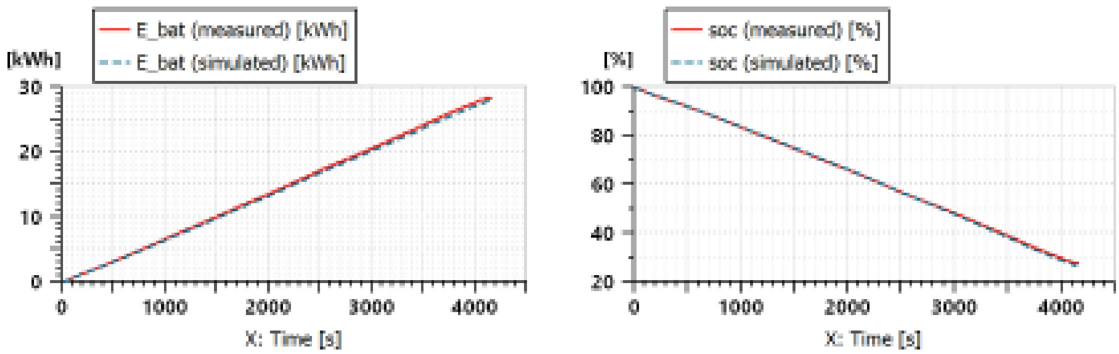

Figure 35 Energy consumed and SOC for level-2

The errors between the simulated values and measured values for the battery energy consumption and SoC (global variables) are calculated in equations (22). These errors are lowers than errors for the level-1 models and prove the accuracy of the models and simulation architecture. In this case, all errors are within the 2% limit.

$$\begin{gathered} nerr(E_{bat}) = \left|\frac{E_{bat,meas} - E_{bat,sim}}{E_{bat,meas}}\right| \cdot 100\% = 1.76\% \\ err(SOC) = |SOC_{meas} - SOC_{sim}| = 0.8\% \end{gathered} \qquad (22)$$

This level-2 model of the battery provides the internal temperature of the battery and this variable is compared with the value from measurements, Figure 36. The simulated temperature is very close to measured value and is explained as the battery of Renault ZOE is air cooled and the cooling is efficient and constant at the high speed relatively constant of the car on the highway. For the model, it was considered a constant convection coefficient. As simulations are usually performed before the battery is build and tested, it is appropriate to consider a constant convection. Thus, the battery temperature has a low impact on the battery behaviour that explain that globally the errors have about the same magnitude than level-1 models.

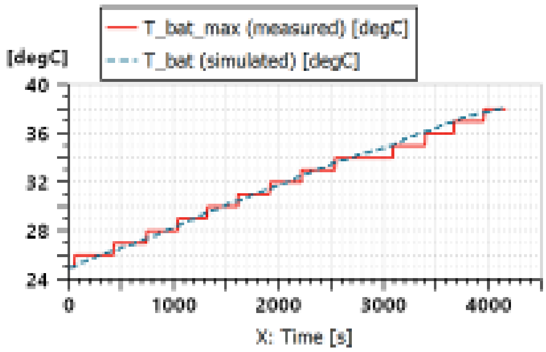

Figure 36 Battery internal temperature simulation (dashed-blue) and measured (red)

5.4.3. Simulation of level-1 configuration model for the urban test scenario

The next scenario simulated is an urban driving test which is very important for a BEV due to frequent charging inputs from braking energy recovery process. Here, the recovered energy from braking is charging the battery every time the car brakes. And besides this recovered energy there is the energy lost with mechanical brake because the electrical brake is not efficient at low speed. An urban cycle where there are many acceleration-brake cycles lead to study the efficiency of the recovered energy. This energy gives more autonomy for the vehicle in urban areas. It was chosen a real urban driving cycle because of the diversity of speed ramps and braking. There are periods where the speed is variable and there are periods where the speed is almost constant. Another difference from previous test is the environment. In the city where was performed the test, there are no slopes and the wind and rolling surface have very little influence comparing with the highway test. Now it is very important to have an accurate model for the recovered energy to have the correct energy consumption. This test with a duration of 2h 26 min is much longer than the previous one, with some stops included.

The same level-1 model presented in Figure 32, with the same parameters was used to simulate this urban cycle. The input variables for the BEV simulation are the same: the total resistive force and the vehicle speed profile (as speed reference for the model) the measured speed of the vehicle.

The results from the simulation compared with corresponded measured variables are presented in Table 6. As for previous tests, the same variables are plotted. On the left column there are variables plotted for the entire test time and on the right column there is a zoom for 200s.

As expected, because of less uncertainties from the environment conditions, the electromagnetic torque and the battery current are closer to the measured values compared with the previous simulations. The difference in battery voltage is similar with the one from previous simulation.

Table 6 Comparison of level-1 simulated and measured parameters for the urban test

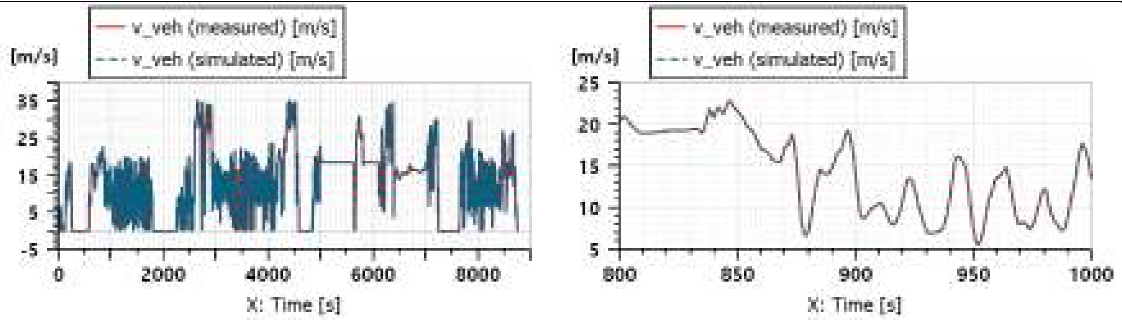

Vehicle speed

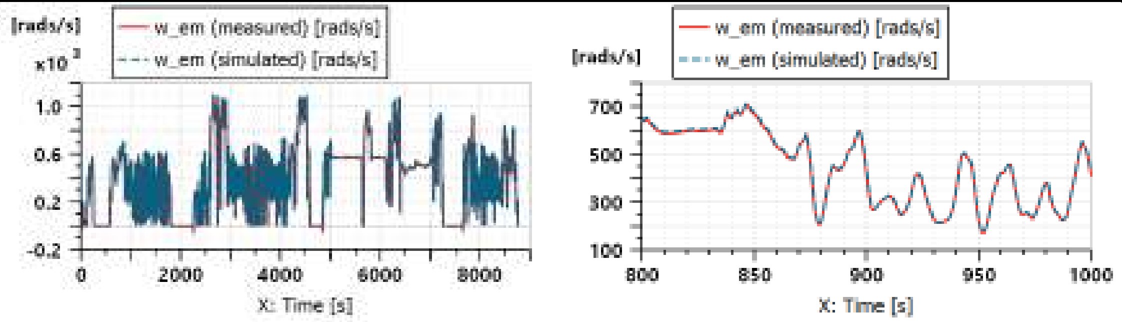

Electric motor speed

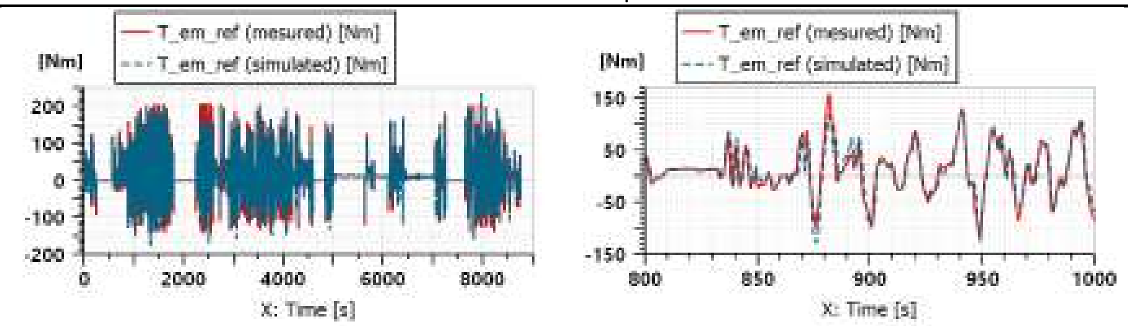

Electromagnetic torque

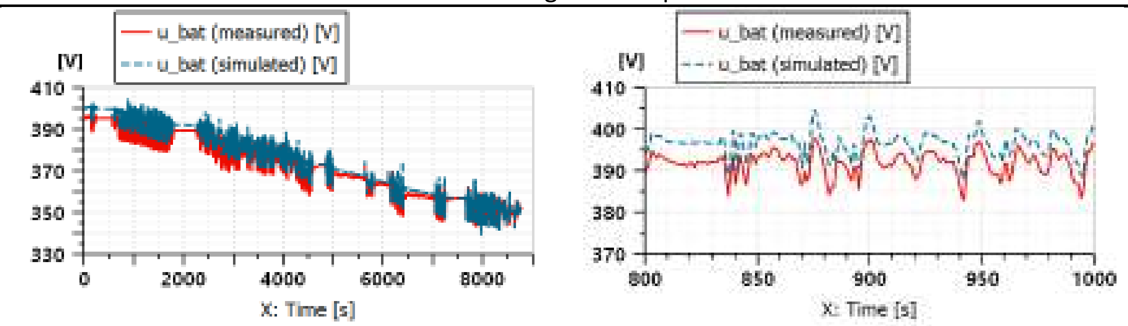

Battery voltage

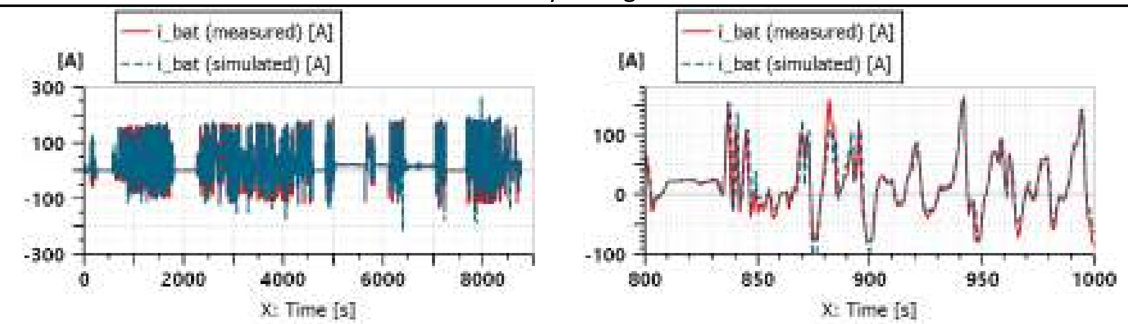

Battery current

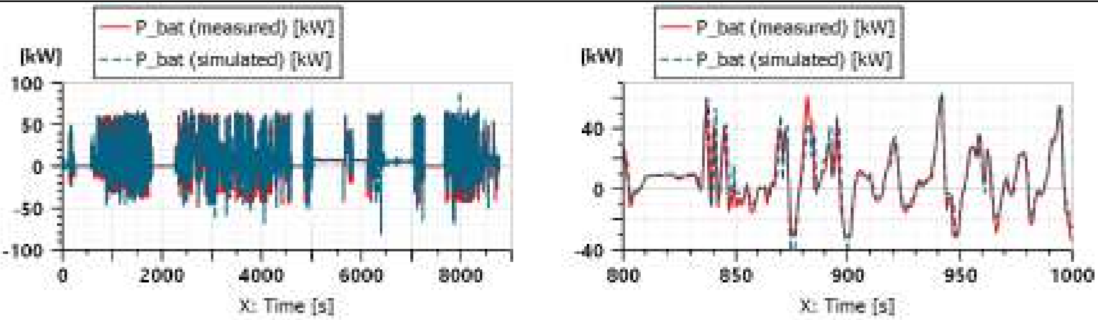

Battery power consumption

The analysis of the local variables, battery voltage and battery current, is done using the same calculation. Thus, for battery voltage the maximum difference between the filtered values of simulated and measured signal on the entire period of the test is 7.04V. This value divided to the average value of the measured voltage for this urban test of 372.5 gives the error for the simulated voltage of 1.88% for entire period. For the zoom window of 200s from the picture on right column we have the difference of 5.24V which divided to the average value of 391.8V on that interval gives the error of the simulated voltage of 1.33%
The analysis the battery current the error related to the rms value of the signal is calculated using the formula form the equation (23):

$$errRMS(i\_bat) = \frac{|RMS(i\_bat_{meas}) - RMS(i\_bat_{sim})|}{RMS(i\_bat_{meas})} \cdot 100 = \frac{|58.91 - 56.26|}{58.91} = 4.49\ \% \qquad (23)$$

For zoom window from 800-1000s of the battery current the error of rms value is 1.21%
For the variables considered for the global evaluation of the accuracy of the simulation, the graphics are in Figure 37.

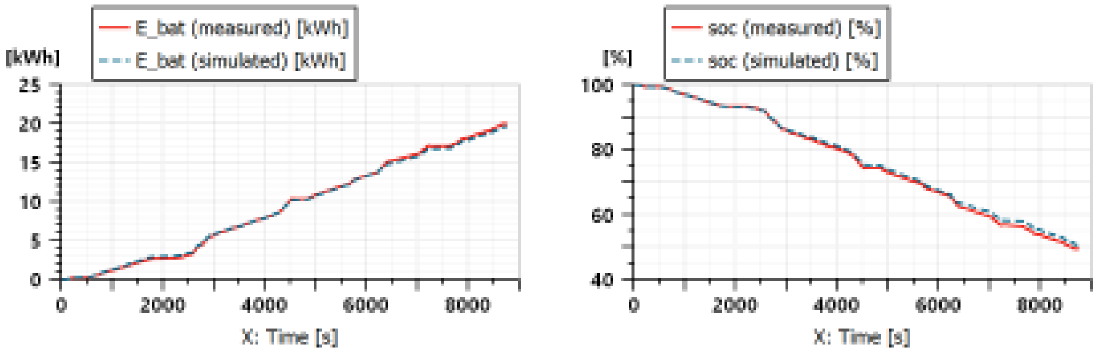

Figure 37 Battery energy consumed and SOC for level-1 model

Overall, the error values for consumed energy and SoC calculated in the same way as for previous test, are quite low in (24). The errors of the global variables are within 2% limit.

$$\begin{gathered} nerr(E_{bat}) = \left|\frac{E_{bat,meas} - E_{bat,sim}}{E_{bat,meas}}\right| \cdot 100\% = 1.88\% \\ err(SOC) = |SOC_{meas} - SOC_{sim}| = 1.24\% \end{gathered} \qquad (24)$$

5.4.4. Simulation of level-2 configuration model for the urban test scenario

For the level-2 model, it was used the model presented in Figure 34. The level-2 model of the battery is connected to level-2 model of the e-drive and the simulation of the urban cycle was performed having the same parameters in the model as for the simulation of the previous highway test. The results are presented in Table 7 having the same parameters on the left column and the same zoom on the right column. Thus, one can compare the simulations results from level-2 model with results form level-1 model. Globally the results are similar with the results from level-1 model.

Table 7 Comparison of level-2 simulated and measured parameters for the urban test

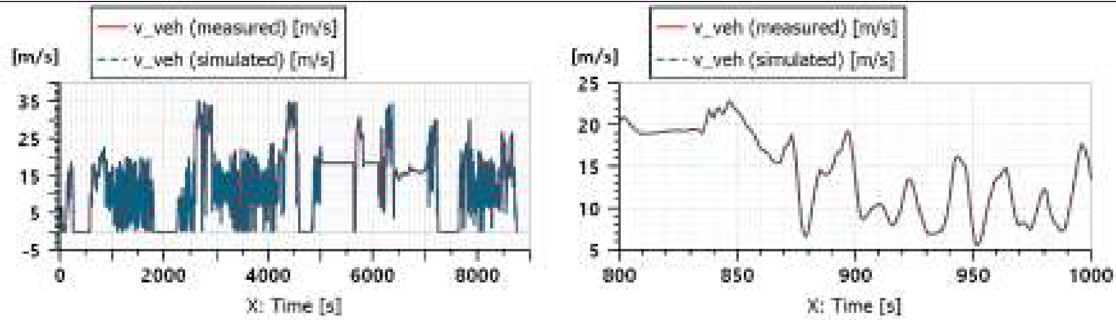

Vehicle speed

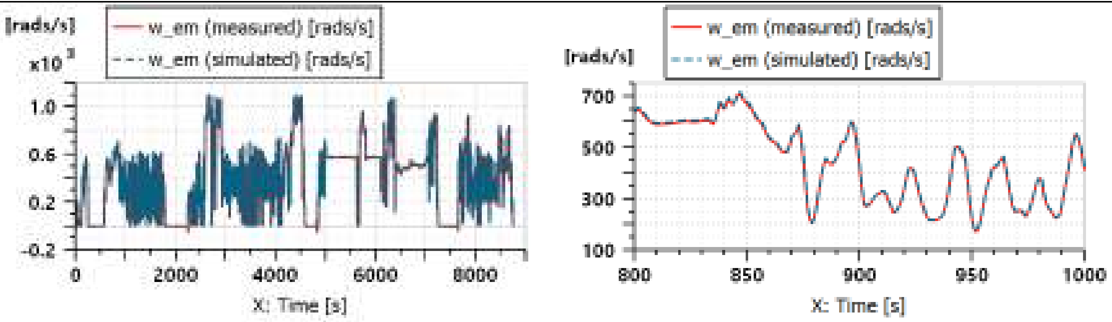

Electrical motor speed

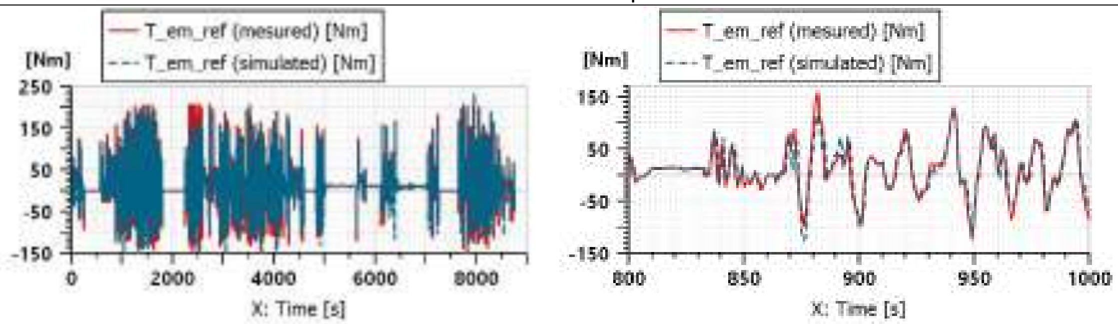

Electromagnetic torque

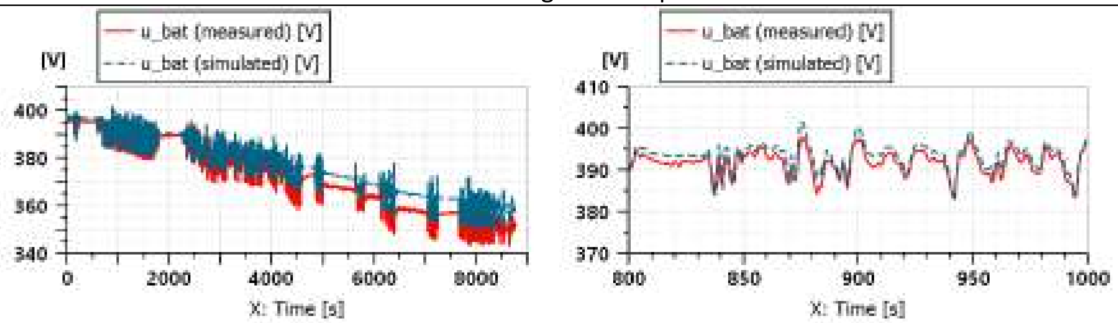

Battery voltage

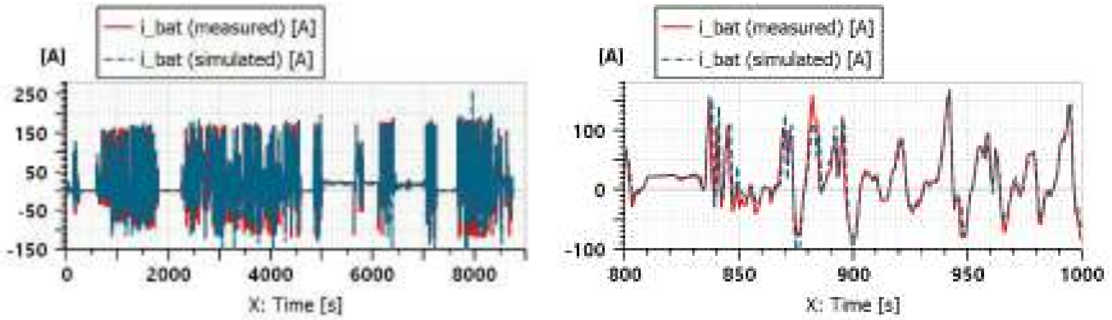

Battery current

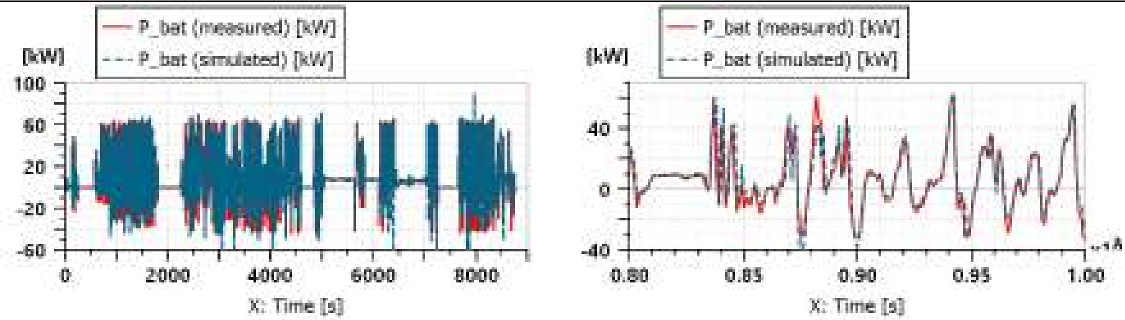

Battery power consumption

The analysis of the local variables battery voltage and battery current is done also. For battery voltage the maximum difference between the filtered values of simulated and measured signal on the entire interval of the test is 11.32V. This value divided to the average value of the measured voltage for this urban test of 372.5 gives the error for the simulated voltage of 3.03% for entire period of the test. For the zoom window of 200s from the picture on right column we have the difference of 2.13V which divided to the average value of 391.8V on that period gives the error of the simulated voltage of 0.54%.
The analysis of the battery current shows the error related to the rms value of the signal (25):

$$errRMS(i\_bat) = \frac{|RMS(i\_bat_{meas}) - RMS(i\_bat_{sim})|}{RMS(i\_bat_{meas})} \cdot 100 = \frac{|58.91 - 56.22|}{58.91} = 4.56\ \% \qquad (25)$$

For zoom window from 800-1000s of the battery current the error of rms value is 2.64%
For this urban test, the battery temperature from simulation is close to measured values but not so precise as during highway test because the cooling of the battery is variable with the speed of the vehicle. The values of the temperature are presented in Figure 38.

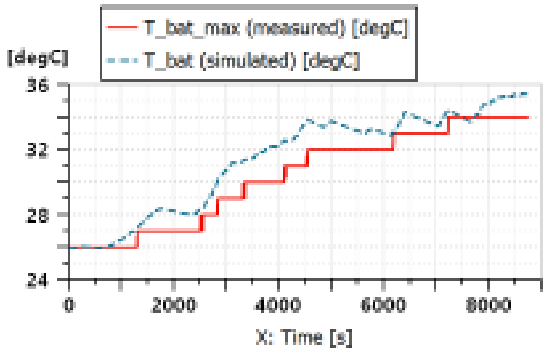

Figure 38 Battery internal temperature simulation (dashed-blue) and measured (red)

The energy consumption and the SOC for level-2 simulation are compared with measured data (Figure 39). They are closer to the measured data as they were in the case of level-1 simulation.

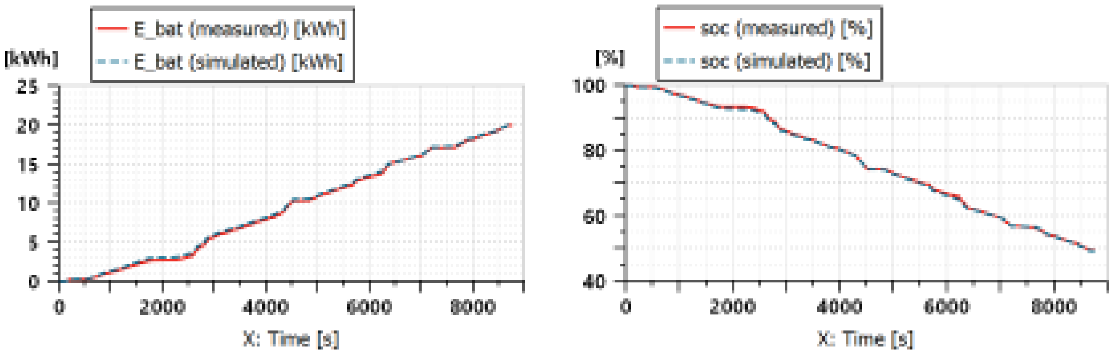

Figure 39 Battery energy consumed and SOC for level-2 model

The errors for energy consumption and the SOC (Figure 39) are quite low within the 2% limit as they are calculated from equation (26). It is reminded that any variation within the 2% error range has no real signification due to the measurement accuracy.

$$nernerr(E_{bat}) = \left|\frac{E_{bat,meas} - E_{bat,sim}}{E_{bat,meas}}\right| \cdot 100\% = 0.51\%$$
$$err(SOC) = |SOC_{meas} - SOC_{sim}| = 0.30\% \qquad (26)$$

If we cannot conclude of the increase of the accuracy at the system level, these detailed models lead to more information such as the battery temperature. However, the degree of the details in these models is done by the maturity of the car project at that moment and it is not possible to use the most detailed model until you have the final parameters of the battery and e-drive.

We can conclude after all simulations that errors for the local variables (battery voltage and battery current) are lower than 6% and errors for the global variables (consumed energy and SoC of the battery) are lower than 3% whatever model was used and whatever test cycle was simulated. The highest errors were for the battery current which is related directly with the resistive forces. As explained before, there are uncertainties of the environment which were not taken into account and contribute to the resistive forces. These low values of errors show the precision of the models and the flexibility of the simulation architecture.

5.4.5. Computation time of the stand-alone and cloud-computing solutions

All simulations were computed on a stand-alone computer but also using a cloud computing solution developed by SISW [PANDA D4.2]. The integration method used was Runge-Kutta with the standard optimisation of the integration step from Simcenter Amesim©. The computation times for all simulation presented in subsection § 5.4 are compared in the following paragraphs.

Highway driving cycle
For the simulation based on level-1 models, the total CPU time was about 20.5s for this highway driving cycle of 1h 10min in stand-alone simulation (Figure 40.a). For the cloud computing simulation, the total CPU time was about 33s, that is 61% higher than for stand alone.
For the simulation based on level-2 models, the total CPU time was about 51.5s for this highway driving cycle in stand-alone simulation (Figure 40.b). For the cloud computing simulation, the total CPU time was about 90s, that is 75% higher than for stand alone.

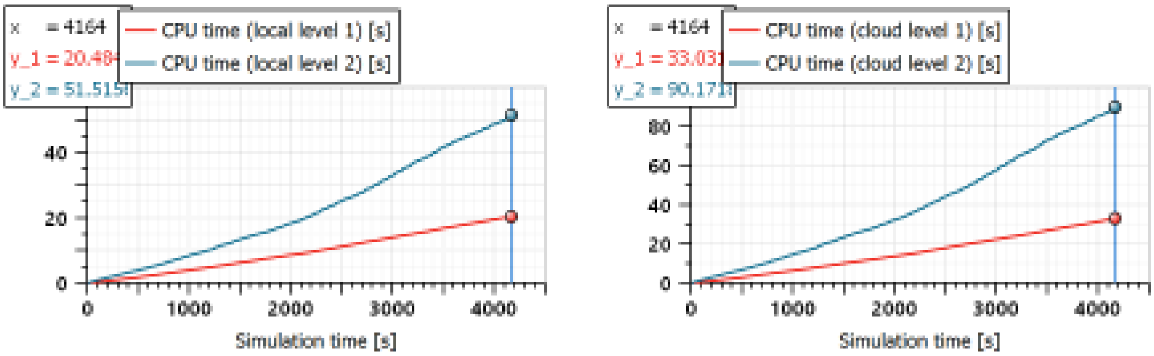

(a) CPU time on stand-alone computer (b) CPU time on cloud computing solution

Figure 40 CPU time as a function of total simulation time for BEV level-1 and level-2

Urban driving cycle

The total CPU simulation time for this urban test with level-1 models is 39s on a stand-alone computer as the total test time is about twice as the simulation time of the highway test (Figure 41.a). For the same simulation on cloud computing solution, the CPU time is about 59.5 seconds (Figure 41.b), that means 53% higher than on the stand alone computer.

The total CPU simulation time for this urban test with level-2 model is 129s on the stand-alone computer, as expected, because the urban test time is longer than highway test time. It can be noticed in Figure 41.a that the variation of the CPU time is not constant because there is an optimisation of the simulation step for periods with low variation of the variables. Regarding the CPU time for cloud computing for level-2 model, it was about 226s that means 75% higher than for the stand alone simulation (Figure 41.b).

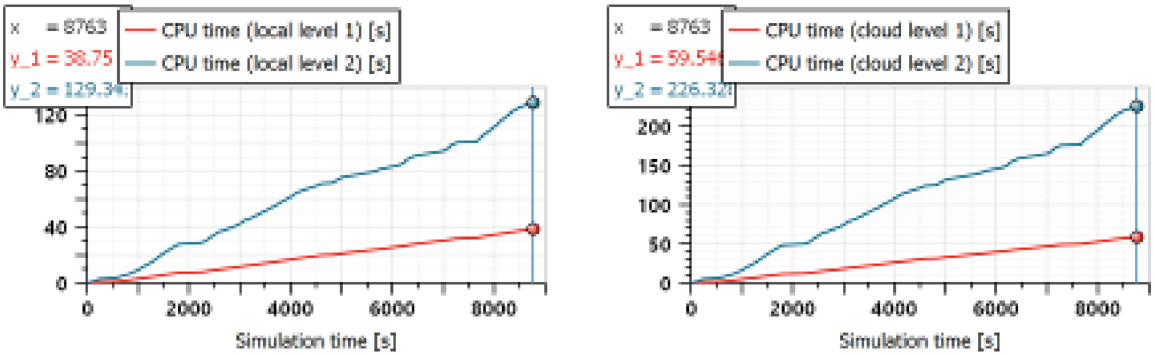

(a) CPU time on stand-alone computer (b) CPU time on cloud computing solution

Figure 41 CPU time as a function of total simulation time for BEV level-1 and level-2

Global comparison of computing solutions

Finally, we notice that for level-1 models, the cloud computing CPU time was 61% higher for highway simulation and 53% higher for urban simulation. For level-2 models, the cloud computing CPU time was 75% higher for highway simulation and 75% higher for urban simulation. There is no clear correlation between the CPU time of the two computing solutions, but we can count on a CPU time lower than twice the CPU time on the stand-alone computer. It is not the purpose of this report to present a detailed analysis of the comparison of computing solutions. It is just an example of the figures someone must take into account when it is chosen a computing solution.

For level-2 model, this the CPU time was 51.5 s for the highway driving cycle and 129s for the urban driving cycle (see Figure 40.b and Figure 41.b). The rate between these periods is 129/51.5=2.50 and the real test time rate is 2h 26 min /1h 10m=2.08. For level-1 models, the simulation time rate is 39/20.5=1.89. Thus, it can be concluded that there is no correlation between the real test time and simulation time.

For information, Table 8 contains the main technical specifications of the two computing solutions used for these simulations. It is to be noticed that the cloud computing solution is a lower cost one, as it is only for the demonstration of the methodology. If a higher cost cloud computing solution is chosen, simulation time will be much lower.

Table 8 Technical specifications of computing solutions used

Stand-alone computer specifications	**Cloud computing specifications**
Processor: Intel Core I7-9850H @ 2,60GHz Installed memory (RAM): 32,0 GB Operating system: Windows 10 Enterprise	Processor: Intel Xeon E5-2666 v3 @ 2,90GHz Installed memory (RAM): 15,0 GB Operating system: Windows Server 2012 R2

Global comparison of simulation and experimentation time

For the urban cycle as the SoC decreased from 100% to 50% in two hours and a half. Based on the results of the real test, we can assume the battery will be almost fully discharged in about 5 hours. More, together with shared car instrumentation and test preparation, one person/day is needed. For the simulation, we count to less than 30 minutes to run the analysis, post-process and prepare the report. Compared with one workday for measured the same test it can be notice the advantage of using simulations instead of experimental tests whenever it is possible.

Let us assume that 1 engineer is in charge of the driving test for energy consumption evaluation of the BEV, and a working day of 8h. In the case of real driving test, the engineer will test a unique driving cycle (with the need of charging the vehicle in the night). It should be noticed that a technician will also be required. In the case of simulated driving cycles, the engineer will provide 16 tests varying the driving conditions during the day. Of course, automatic simulation process could be developed to gain more time. Thus, the testing time will be dived by 16 with accurate simulation model. The idea in not to replace any real driving test but to replace them as much as possible to save time to market in the development phase.

6. LCA Indicators for e-drive of the studied BEV

The aim of this section is to show how the developed simulation tool can contribute to evaluate the LCA of a studied vehicle during its development phase. Most of the LCA studies are conducted as post-assessment of existing vehicles. In PANDA, a forward-looking or prospective approach is considered [PANDA D1.7]. For example different choices of subsystems or usages can be evaluated in terms of LCA using the simulation tool.

Thus, the objective of this section is not to provide an accurate and realistic LCA of the Renault ZOE, but to show how the PANDA methodology can be useful in the pre-LCA analysis. The climate change indicator (Global Warming Potential, in CO2 equivalent) is only considered in this report, but other LCA indicators can be studied using the same approach.

A general framework is first defined with the definition of the perimeter and assumptions. Then, the LCA indicators of the battery (WP2) and of the e-drive (WP3) are reminded. Finally, the LCA of the complete vehicle is discussed from different driving cycles.

6.1 Framework of the study

Life Cycle Assessment (LCA) is an evolving method applied for assessing the potential environmental effect caused by certain processes or products (in this case BEVs). All materials and energy consumption used for a product, will be evaluated for all life cycle stages (Figure 42), from the raw materials extraction, to manufacturing until the use and end of life phases. This evaluation is needed to quantify the product's lifetime impact in terms of emissions and waste. LCA encompasses risk estimation and environmental impact assessment that can be implemented at each phase of the life cycle relying on International Standards ISO 14040 and ISO 14044.

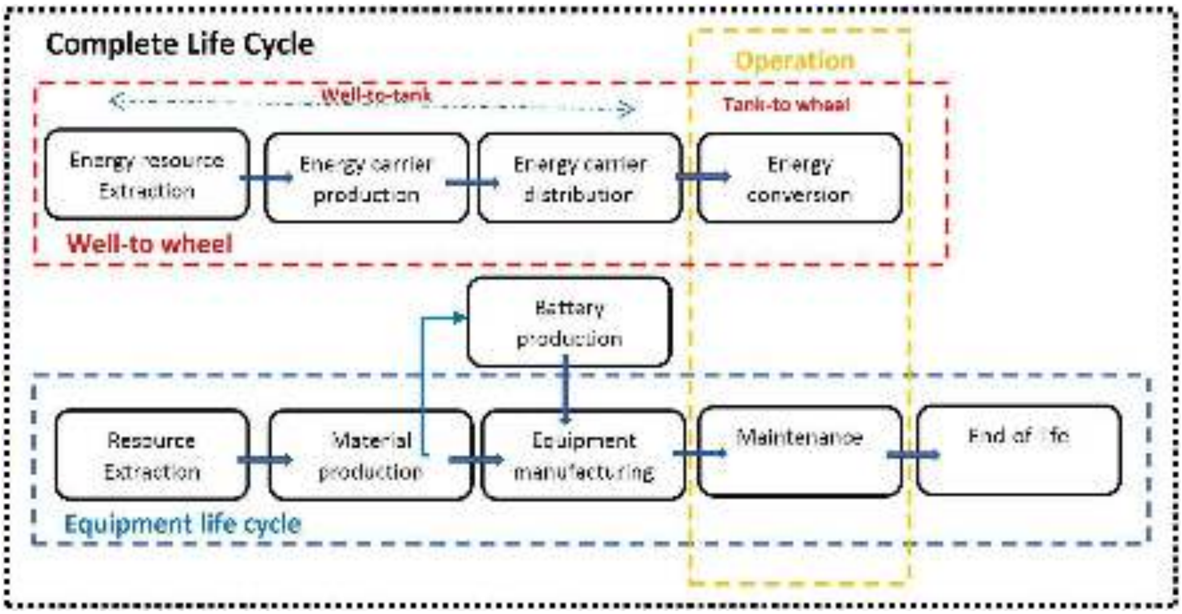

Figure 42 Simplified representation of system boundary of vehicle LCA, adapted from [Nordelöf 2014]

There are several LCA indicators related to human health, natural environment and natural resources. [Huijbregts 2017]. As this report is dedicated to the demonstration of the interest of simulation tool for forward LCA, the main indicator is only considered. It is the Greenhous gazes (GHG) associated to climate change (Global Warming Potential) and expressed in CO_2 equivalent. Other indicators could be computed in the same philosophy.

Moreover, as LCA is a huge process requiring a lot of data, we will focus on the methodology and not on the results. In order to have a reference point, the figures of Nissan Leaf 2010 for a NEDC is considered [Hawkins 2013], see Table 9.

Table 9 Main parameters of the reference vehicles and the studied vehicle

	Nissan Leaf 2010	**Renault ZOE 2017 (Q90)**
Vehicle mass	1 500 kg	1 470 kg
Li-ion battery	24 kWh (MNC)	41 kWh (MNC)
Electrical machine	81 kW (PMSM)	61 kW (WR-SM)
Life-time distance	150 000 km (NEDC)	150 000 km (NEDC)

From these studies, the climate change (Global Warming Potential) indicator can be extracted between the usage (electricity consumption and production), the battery production and end-of-life, the e-drive production and end-of-life, the glider (all vehicle parts except the e-drive and the battery). The climate change indicator for Nissan Leaf of the different parts are presented in Table 10.

Table 10 Climate change indicator of the reference vehicles

	Nissan Leaf 2010	
e-drive	1 305 kg CO2 eq	5%
battery	4 568kg CO2 eq	16%
glider	7 178 kg CO2 eq	25%
Usage (well to tank)	15 575 kg CO2 eq	54%
Total	28 625 kg CO2 eq	100%

6. 2. LCA of the battery and the e-drive

In this subsection the indicator of the manufacturing phase of the battery and the e-drive, are calculated from the LCA studies conducted in WP2 and WP3. As the manufacturing phase is independent of the usage, these indicators will be used as fixed value in the global indicator of the complete vehicle.

The LCA indicators for Renault ZOE were developed in WP2 for the battery by VUB [PANDA D2.4]. The ZOE battery is 41 kWh of MNC Li-ion. It is the same battery type than the Nissan Leaf. The climate change indicator has been computed for 140 000 km and including the usage phase. From these results, we can extract the manufacturing phase with a ratio of 129 kg CO2 / kWh that leads to a total of 5 284 kg of CO2. It can be noted that the Nissan Leaf use a 160 kg CO2 / kWh ratio for a 24 kWh but from a 2010 technology. We can conclude that the figures reported in WP2 are in agreement with classical figures.
It can be noted that 75% of this indicator is due to the cell manufacture [PANDA D2.4]. A significant reduction of the cell manufacture can thus strongly reduce this indicator. Moreover, a second use of the battery (e.g. second life for stationary application) can share this CO_2 between the vehicle and another application.

The LCA indicators for Renault ZOE were developed in WP3 for the e-drive by UTCN [PANDA D3.4]. The ZOE e-drive is composed of a 65 kW wound rotor synchronous machine (WRSM), a 3-leg voltage source inverter and a field chopper. The climate change indicator has been computed for 200 000 km and include the usage phase. From these results, we can extract the manufacturing phase indicator with a ratio of 6 kg CO2 / kW that leads to a total of 381 kg CO2. The Nissan Leaf use a 21 kg CO2 / kW ratio for a 82 kW PMSM. Moreover, from in internal report of Renault [ZOE-LCA 2012], the climate change indicator of the e-drive was estimated to 10 kg CO2 / kW but for technology of 2012 (ZOE R210). We can conclude that the figures reported in WP3 are in agreement with classical figures. The dispersion can be explained by the uncertainties of the ratio of each material (from 30% to 50%). The impact of the permanent magnet seems very important for the e-drive.

It can be noted that 75% of this indicator is due to the winding. Optimal machine design could thus decrease this indicator [PANDA D3.4]. But for PMSM, it is sure that the main contributor to LCA are the permanent magnets.

6.3. LCA of the studied BEV

The principle of the computation of the climate change indicator developed in $ 6.1 for the reference vehicles is extended to the studied BEV. Unfortunately, no in-depth analysis has been provided for the glider. For this part, we will use the value of the glider estimated for Renault ZOE 2012 in an internal report of Renault [ZOE-LCA 2012]. In this report, the climate change indicator of the glider is estimated at 4171 kgCO2 for Renault ZOE R210. Even though this figure is not the real one of the studied vehicle, it can be assumed of the right order for the studied Renault ZOE Q90, where the most important change is related to the battery.

For the life-time distance, 150 000 km is selected. For the electricity production, the European mix of 2016 is selected that leads to 449 gCO2 /kWh including the distribution losses [PANDA D1-7]. The developed simulation tool can thus compute the energy consumption for the considered driving cycle in kWh / km. The climate change of the usage can thus be directly computed. First a NEDC is considered as for the two reference vehicles. This base case is described in Table 11. As explained before, only the glider has not been derived from a detailed study. Anyway, the total climate indicator is of the same order of magnitude of the ones of the reference vehicles with a more important for the battery which is the biggest in the studied vehicle.

Table 11 Climate change indicator of the studied vehicle for the base case (NEDC/150 000 km/Euro Mix)

Renault ZOE	kg CO2 eq	
e-drive	381	2%
battery	5 284	28%
glider	4 171	22%
Usage (well to tank)	9 052	48%
Total	18 928	100%

The simulation tool can integrate other components with other manufacturing indicators and also their weight (impact on the energy to move the car and thus on the usage indicator). Another possibility is to consider the impact of the real driving cycles measured by Renault (Table 12). In these cases, only the usage indicator changes. It can be observed that real driving cycles increase the part of the usage indicator from 48% up to 61%, and thus decreases the other parts, including the battery indicator. As well known, NEDC has the lowest indicator.

Table 12 Climate change indicator of the studied vehicle for different driving cycles

Renault ZOE	Real urban (kgCO2eq)		Real highway (kgCO2eq)	
e-drive	381	2%	381	2%
battery	5 284	24%	5 284	21%
glider	4 171	19%	4 171	17%
Usage (well to tank)	12 460	56%	15 154	61%
Total	22 295	100%	24 989	100%

Another study can be related to the battery second use. Generally, in electric vehicles, the battery is replaced when its capacity loses 20% to 30% from its initial value [Martinez 2018]. In stationary applications, the remaining capacity can be used up to a degradation of 60% or more. In a simplistic point of view, if we consider that the manufacturing impact is shared equally by the vehicle and the secondary application, the climate change of the battery can be divided by 2 in the base case. Once again, this subsection do not aim to provide realistic study in battery second life, but to show haw this aspect can be considered. The total climate change indicator is thus reduced and the part of the battery is only 16% (instead of 28%) in the base case with NEDC and 150 000 km (Table 13).

Table 13 Climate change indicator of the studied vehicle for the base case with battery second use

Renault ZOE	**NEDC / 150 000 km**	
e-drive	381 kg CO2eq	2%
battery	2 642 kgCO2eq	16%
glider	4 171 kgCO2eq	26%
Usage (well to tank)	9 092 kgCO2eq	56%
Total	16 286 kg CO2eq	100%

These simple cases cannot have accurate value due to the considered assumptions. But they demonstrate that the simulation tool can contribute to the life cycle analysis of the studied vehicle in the early phase of development. Other LCA indicator can be studied in the same way.

7. Discussion and Conclusions

7.1 Discussion

Simulation results from this document represent the virtual testing for the selected BEV, Renault ZOE. Some experimental tests have been achieved on a real vehicle for different driving cycles. These results were used for individual validation of the models of electrical powertrain components: battery, e-drive and car body. With these validated models, the simulation results of the complete vehicle were compared with measurements on the real vehicle. The results presented in this document were considered representative for the purpose of the PANDA project: to validate virtual tests of the BEV and to prove the efficiency of proposed model organisation applied on a real BEV. Each model was validated before by partners in charge with their development and in this document, there is the validation of simulations of the global vehicle and the efficiency of multi-level simulation.

7.2 Conclusions

This report presents the virtual testing of the BEV with validation on measured test data of Renault ZOE. It contains a brief description of multi-level models developed. Then models are connected to compose the architecture of the BEV and the results from the simulations are compared with measurements from tests. A vehicle Renault ZOE was tested in several scenarios in order to cover most use cases of a car without working close to the limits. These scenarios were chosen to cover general use cases and the tests were done in real traffic in order to have uncertainties in measurements for a severe validation of the simulations.

The purpose was achieved, simulations proved a high accuracy with a maximum of 3% error for cumulative variables– total energy consumption and state of charge of the battery. There were simulated and validated the battery temperature, torque and speed of the electric motor, voltage and current form the battery. An analysis was done on subsystem variables, battery voltage and battery current and it was proved that the error was lower than 6% for any of the models used on any of the tests simulated. These results demonstrate the reliability of the developed models, which were organized according to the EMR rules.

The report proved that the model organization chosen for PANDA project can be implemented in different software tools. Thus, models were developed for Matlab-Simulink© environment and Simcenter Amesim© environment using the same EMR formalism. By using the dedicated library developed in Simcenter Amesim© the implementation of the models was much easier and models are visual closer to EMR general structure. This result demonstrates the portability of the PANDA methodology based on the EMR formalism.

Multi-level simulations of the BEV have been validated by test measurements proved the flexibility of the architecture provided by model organisation. Having the same input and output ports models can be changed and connected very easy to the simulation architecture. Simulations were performed using Simcenter Amesim© using dedicated EMR library developed. Thus, level-0 validated model of the BEV was presented in section 4 where it was compared with measurements from mixed cycle test. Level-1 and level-2 models of the BEV were presented in section 5, where there were compared with measurements form highway test and urban test. In this report there were presented three levels of simulation of the BEV validated with measurements form different tests. Simulation results were close to measured variables on the vehicle for all tests, proving the accuracy of the models and global architecture for all three levels of simulation. According to the maturity of a car project, during the development phase it can be used the model where the parameters are available. These results demonstrate the flexibility of the PANDA methodology based on the EMR formalism.

The CPU simulation time obtained is quite small for the measured test time and shows the efficiency for the developed models thanks to the respect of the causality [Husar 2019]. Simulations of level-1 and level-2 models were analysed. They showed how the differences between the complexity of the models of BEV have impact in simulation time and they demonstrate the importance of choosing the right level-for the simulation for a specific purpose during the BEV development. The cloud computing solution developed during project was also used for the same simulations to prove the efficiency of the solution. The small simulations time give confidence for the next step of the project – real time simulations. These results demonstrate the use of the two simulations option of PANDA: stand alone or cloud computing.

Finally, an LCA study has been proposed on the climate change indicator and the simulation tool has provided the usage part as a function of the driving cycle. If the results have no significant values due to the strong assumptions, they demonstrate the interest to consider LCA in the early phase of development thanks to the developed simulation tool.

8. Deviations from Annex 1

There are no deviations with respect to the description of work. In terms of timing, the deliverable has been delayed from M24 to M25 in order to include the level-2 model for e-drive for WRSM. Models for WRSM were not presented in [PANDA D3.1] and they were developed and validated between M13-M24.

9. References

[Baert 2012] J. Baert, S. Jemei, D. Chamagne, D. Hissel, S. Hibon, D. Hegy, "Energetic Macroscopic Representation of a Naturally-Aspirated Engine coupled to a salient pole synchronous machine," IFAC Proceedings Volumes, Volume 45, Issue 21, 2012, pp. 435-440

[Boldea 2005] I. Boldea, S. A. Nasar, "Electric drives," Second Edition, CRC Press, 2005

[Bouscayrol 2012] A. Bouscayrol, J. P. Hautier, B. Lemaire-Semail, "Graphic Formalisms for the Control of Multi-Physical Energetic Systems", Systemic Design Methodologies for Electrical Energy, tome 1, Analysis, Synthesis and Management, Chapter 3, ISTE Willey editions, October 2012, ISBN: 9781848213883.

[EMRwebsite 2019] EMR website, http://www.emrwebsite.org/ (consulted 2019)

[German 2020] R. German, S. Shili, A. Desreveaux, A. Sari, P. Venet and A. Bouscayrol, "Dynamical Coupling of a Battery Electro-Thermal Model and the Traction Model of an EV for Driving Range Simulation", IEEE transactions on Vehicular Technology, Vo. 69, no. 1, January 2020, pp. 328-337

[Hautier 2004] J.P. Hautier, P.J. Barre, « The causal ordering graph – A tool for modelling and control law synthesis", Studies in Informatics and Control Journal, vol. 13, no. 4, pp. 265-283; 2004.

[Huria 2012] T. Huria, M. Ceraolo, J. Gazzarri, and R. Jackey, "High Fidelity Electrical Model with Thermal Dependence for Characterization and Simulation of High Power Lithium Battery Cells," IEEE Int. Electr. Veh. Conf., pp. 1–8, 2012.

[Jaguemont 2015] J. Jaguemont, L. Boulon, and Y. Dubé, "A comprehensive review of lithium-ion batteries used in hybrid and electric vehicles at cold temperatures," Applied Energy, vol. 164, pp. 99–114, 2016.

[Hawkins 2013] T. R. Hawkins, B. Singh, G. Majeau-Bettez, A. Hammer Strømman, "Comparative Environmental Life Cycle Assessment of Conventional and Electric Vehicles" *Journal of Industrial ecology*, Vol. 17, no. 1, February 201, pp. 53-64.

[Huijbregts 2017] M.A.J.Huijbregts, Z.J.N. Steinmann, P.M.F. Elshout, G. Stam, F. Verones, M. Vieira, M. Zijp, A. Hollander, R. van Zelm, R., 2017. "ReCiPe2016: a harmonised life cycle impact assessment method at midpoint and endpoint level", International Journal of Life Cycle Assessement, vol. 22, 2017.

[Husar 2019] C. Husar, M. Grovu, C. Irimia, A. Desreveaux, A. Bouscayrol, M. Ponchant, P. Magnin, "Comparison of Energetic Macroscopic Representation and structural representation on EV simulation under Simcenter Amesim©", IEEE-VPPC'19, Hanoi (Vietnam), October 2019 (Siemens Software and L2EP within the framework of the H2020 PANDA project.

[Martinez 2018] E. Martinez-Lasernaa, I. Gandiagaa, E. Sarasketa-Zabalaa, J. Badedab,c,d, D.-I. Stroee, M. Swierczynskie, A. Goikoetxeaf, 'Battery second life: Hype, hope or reality? A critical review of the state of the art', Renewable and Sustainable Energy Review, vol. 93, October 2018, pp. 701,718

[Messagie 2017] M. Messagie, "Life Cycle Analysis of the Climate Impact of Electric Vehicles", Transport & Environnement, 2017.

[Nordelöf 2014] A. Nordelöf, M. Messagie, A.-M. Tillman, M.L. Söderman, J. Van Mierlo, Environmental impacts of hybrid , plug-in hybrid , and battery electric vehicles — hat can e learn from life cycle assessment ?", International Journal of Life Cycle Assessment, Vol. 19, pp. 1866–1890, 2014.

[PANDA 2019] A. Bouscayrol, A. Lepoutre, C. Irimia, C. Husar, J. Jaguemont, A. Lièvre, C. Martis, D. Zuber, V. Blandow, F. Gao, W. Van Dorp, G. Sirbu, J. Lecoutere, "Power Advanced N-level Digital Architecture for models of electrified vehicles and their components", *Transport Research Arena 2020*, Helsinki (Finland), April 2020 (within the framework of the PANDA H2020 European Project, GA #824256).

[PANDA D1.1] D. Chrenko, A. Bouscayrol, B. Lemaire-Semail, C. Husar, "PAND D1.2: State-of-the-Art on vehicle simulation and testing", PANDA H2020 GA# 824256, D1.1 Deliverable, public report, May 2019, [Online] Available: https://project-panda.eu/ Accessed January 2020)

[PANDA D1.2] B. Lemaire-Semail, A. Bouscayrol, "PANDA D1.2: Organisation method for virtual and real testing", PANDA H2020 GA# 824256, D1.1 Deliverable, confidential report, February 2020, [Online] Published executive summary available: https://project-panda.eu/ Accessed October 2020)

[PANDA D1.6] V. Blandow, D. Chrenko, "PANDA D1.6 Testing Scenarios", PANDA H2020 GA# 824256, D1.6 Deliverable, confidential report, October 2020, [Online] Published executive summary available: https://project-panda.eu/ Accessed October 2020)

[PANDA D1.7] M.S. Koroma, G. Cardellono, M. Messagie, "Guidelines for forward LCA approach", PANDA H2020 GA# 824256, D1.7 Deliverable, confidential report, December 2019, [Online] Published executive summary available: https://project-panda.eu/ Accessed October 2020)

[PANDA D2.1] J. Jaguemont, C. Husar, R. German, "PANDA D2.1 Multi-level knowledge models of batteries", PANDA H2020 GA# 824256, D1.6 Deliverable, c report, November 2019, [Online] Published executive summary available: https://project-panda.eu/ Accessed October 2020).

[PANDA D2.4] M.S. Koroma, G. Cardellini, M. Messagie, "LCA indicators of NMC batteries", PANDA H2020 GA# 824256, D2.4 Deliverable, confidential report, October 2020, [Online] Published executive summary available: https://project-panda.eu/ Accessed October 2020).

[PANDA D3.1] M. Ruba, C. Husar, "PANDA D3.1 Multi-level knowledge models of e-drives", PANDA H2020 GA# 824256, D1.6 Deliverable, c report, November 2019, [Online] Published executive summary available: https://project-panda.eu/ Accessed October 2020).

[PANDA D3.4] A.Tintelecan, A.Constantinescu, "LCA indicators of e-drives", PANDA H2020 GA# 824256, D1.6 Deliverable, confidential report, October 2020, [Online] Published executive summary available: https://project-panda.eu/ Accessed October 2020).

[PANDA D4.1] C. Husar, "PANDA D4.1 Simulation platform and library", PANDA H2020 GA# 824256, D1.6 Deliverable, confidential report, February 2020, [Online] Published executive summary available: https://project-panda.eu/ Accessed October 2020)

[PANDA D4.2] M. Ciocan, R. Gavril, report "PANDA D4.2 Cloud facilities", PANDA H2020 GA# 824256, D1.6 Deliverable, confidential report, June 2020, [Online] Published executive summary available: https://project-panda.eu/ Accessed October 2020)

[Qiu 2016] C. Qiu and G. Wang, "New evaluation methodology of regenerative braking contribution to energy efficiency improvement of electric vehicles," Energy, Conversion and Management, vol. 119, pp. 389-398, 2016.

[Raia 2019] M. R. Raia, A. Pop and C. Martis, "Scalable abc-Modelling of Permanent Magnet Synchronous Machines for Model Order Reduction," 2019 IEEE Workshop on Electrical Machines Design, Control and Diagnosis (WEMDCD), Athens, Greece, 2019, pp. 83-88

[Rubin 1997] Z. Rubin, S. Munns, J. Moskowa, "The development of vehicular powertrain system modeling methodologies: philosophy and implementation", System Automotive Engineering, paper 971089, 1997

[Ruba 2019] M. Ruba, R. O. Nemes, S. M. Ciornei, C. Martis, A. Bouscayrol and H. Hedesiu, "Digital Twin Real-Time FPGA Implementation for Light Electric Vehicle Propulsion System Using EMR Organization," 2019 IEEE Vehicle Power and Propulsion Conference (VPPC), Hanoi, Vietnam, 2019, pp. 1-6

[Szabo 2009] L. Szabo, D. Fodorean, "Simularea ansamblului convertor-mașină utilizat în sisteme electromecanice," Cluj-Napoca, 2009, U.T. Press, pp.144-158.

|ZOE-LCA 2012] "ZOE Life Cycle Assessment", Renault SAS, Internal report, 2012.

7. Acknowledgement

The author(s) would like to thank the partners in the project for their valuable comments on previous drafts and for performing the review.

Table 14 Project Partners

#	Type	Partner	Partner Full Name
1	UNIV	ULille	Université de Lille
2	IND	SISW	Siemens Industry Software SRL
3	UNIV	VUB	Vrije Universiteit Brussels
4	IND	VEEM	VALEO Equipement Electriques Moteur SAS
5	UNIV	UTCN	Universitatea Tehnica Cluj Napoca
6	SME	TY	Tajfun HIL (Typhoon HIL)
7	-	-	(change of partner)
8	UNIV	UBFC	Université Bourgogne Franche-Comté
9	SME	UNR	Uniresearch BV
10	IND	RTR	Renault Technologie Roumanie
11	SME	Bluways	BlueWays International bva
12	IND	TUV	TUV SUD Battery Testing Gmbh

This project has received funding from the European Union's Horizon2020 research and innovation programme under Grant Agreement no. 824256.

Appendix B – Quality Assurance

As part of the quality assurance procedure:

- The following questions should be answered by all reviewers (WP Leader, peer reviewer 1, peer reviewer 2 and the technical coordinator);
- Questions answered with NO should be motivated. The author will then make an updated version of the Deliverable. When all reviewers have answered all questions with YES, only then the Deliverable can be submitted to the EC.

NOTE: For public documents this Quality Assurance part will be removed before publication.

Question	WP Leader	Peer reviewer 1	Peer reviewer 2	Technical Coordinator
	Cristi IRIMIA	Calin HUSAR	Johannes ROESSNER	Alain BOUSCAYROL
1. Do you accept this deliverable as it is?	Yes	Yes	Yes	Yes
2. Is the deliverable completely ready? If not, please indicate and motivate required changes.	Yes	Yes	Yes	Yes
3. Does this deliverable correspond to the DoW?	Yes	Yes	Yes	Yes
4. Is the Deliverable in line with the PANDA objectives?	Yes	Yes	Yes	Yes
a. WP Objectives?	Yes	Yes	Yes	Yes
b. Task Objectives?	Yes	Yes	Yes	Yes
5. Is the technical quality sufficient?	Yes	Yes	Yes	Yes

Appendix C – Abbreviations / Nomenclature

Table 15 List of Abbreviations / Nomenclature

Symbol / Shortname	
BEV	Battery Electric Vehicle
BMS	Battery Management System
CPU	Central Processing Unit
ECU	Electronic Control Unit
EMR	Energetic Macroscopic Representation
EVC	Electric Vehicle Computer
LCA	Life Cycle Assessment
NEDC	New European Driving Cycle
PEB	Power Electronics Block
PMSM	Permanent Magnet Synchronous Motor
PWM	Pulse Width Modulation
SoC	State of Charge
WLTP	Worldwide Harmonised Light Vehicle Test Procedure
WRSM	Wound Rotor Synchronous Machine